International Spring School on Forefront Alloys and Advanced Materials for Extreme Conditions

15 – 17 May 2017

Sardinia, Italy

Advanced Ceramics for Energy and Nanomechanical Methods for in-situ characterization and residual stress estimate

Antonio Rinaldi (ENEA)

Table of Contents

1. On ceramics for Nuclear and Concentrated Solar Power
2. Residual Stresses and In-Situ Characterization

PART 1
On ceramics for Nuclear and Concentrated Solar Power

PART 1 On Ceramics for Nuclear and Concentrated Solar Power

A nuclear overview

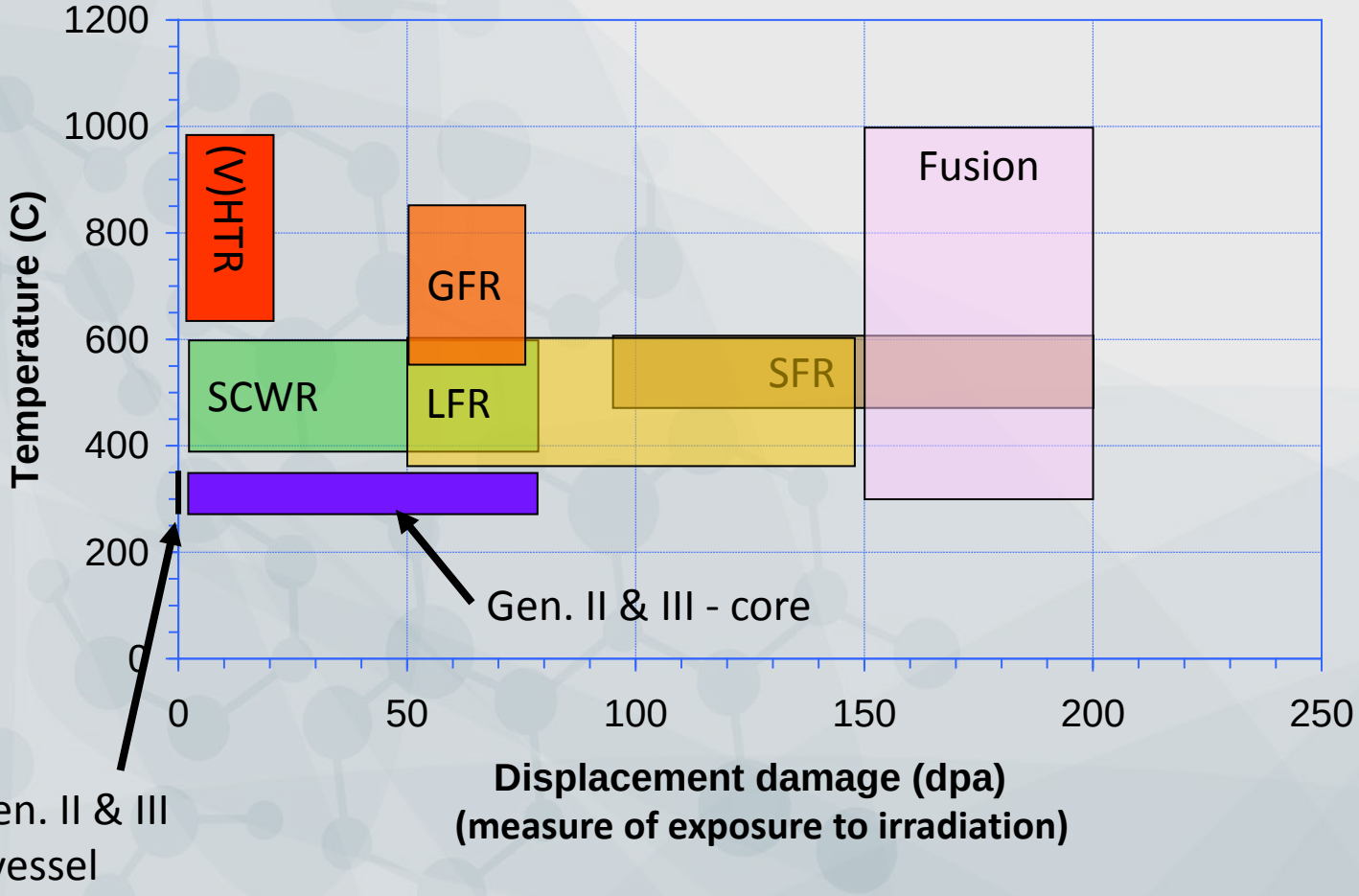

PART 1 On Ceramics for Nuclear and Concentrated Solar Power

A nuclear overview

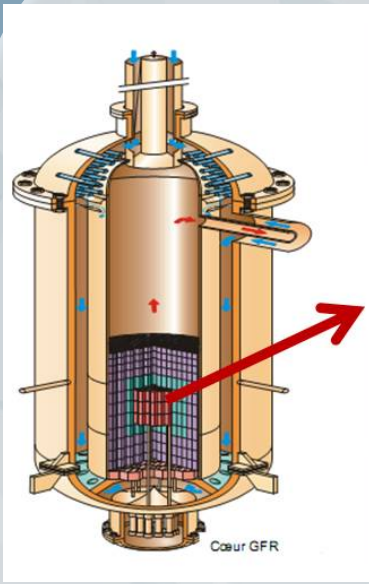

Temperature
- Normal: 600-1000 °C
- Off –normal: 1600-2000 °C

Fast neutron irradiation dose
- Up to 80 dpa in SiC

Mechanical stress/strain
- Up to 100 MPa/0.5%

High T impure helium coolant
- 7 Mpa, 70 m/s

GFR assets: Energy efficiency, Generation of process heat

GFR clad requirements for safety

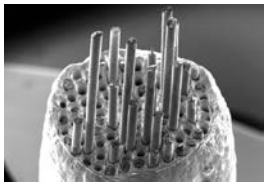

No melting
Leak tightness
Structural integrity
Heat transfer

SiC_f/SiC is the only material that fulfills most requirements

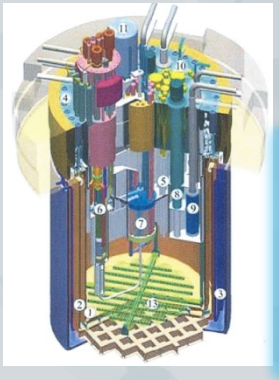

LFR assets:
Inherent high safety features

LFR materials issues
Corrosion/erosion of materials in lead implying strict control of temperature, dissolved oxygen & speed.

- Material innovation is required for **pump impeller**
- Very emerging materials with promising capabilities are **MAX phases** (ternary carbides, e.g. Ti_3SiC_2)

PART 1 On Ceramics for Nuclear and Concentrated Solar Power

A nuclear overview: a success story

Two pilot projects addressed for the fabrication of hermetic SiCf/SiC clad sections

1- Design of promising SiCf/SiC microstrutures based on key property requirements; feasibility of fabricating clad sections out of them

2- Development of hermetic measures (lining/coating) for SiCf/SiC clads; feasibility of incorporating them into clad format

Objective of a French national program lead by CEA and pursued independently

The hybrid "sandwich" clad

CEA patent

GFR fuel cladding

- SiC_f/SiC sandwich clad technology is a breakthrough from a French national programs lead by CEA
- It guarantees **leak-tightness** for increased **safety**

PART 1 On Ceramics for Nuclear and Concentrated Solar Power

A nuclear overview: a success story

Development of **predictive behavioural models**

In MatISSE, development of multi-scale experimental tools: (CEA, UOXF, UNIMAN)

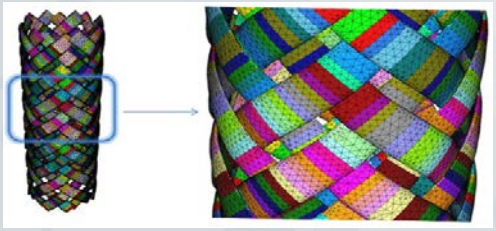

Credit: J. Marrow (U.OXFORD)

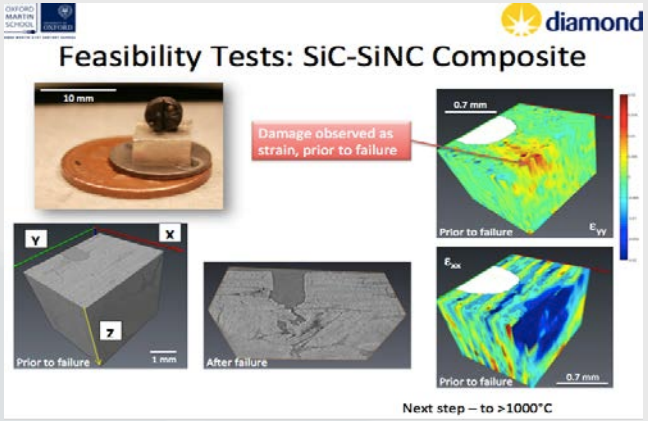

Task-force ongoing in EERA-JPNM for:

- Modelling strategies for the Influence of Microstructure on Elastic and Thermal properties in CMC Clad for GFR applications (**UOXF**, CEA, UNIMAN, ENEA….) **ready to be circulated**
- **Jo**ints for tight sealing **S**iC/SiC **T**ubes of GFR p**I**n-fuel **c**lad: **C**ombined experimental/modelling approaches (**POLITO**, ENEA, SCK.CEN, KUL, UTD..) **under consolidation**
- Modelling of irradiation behaviour of SiCf/SiC and MAX-phases

For more: EERA – JPNM – SUPBPROGRAM 3

PART 1 On Ceramics for Nuclear and Concentrated Solar Power

There is an ongoing effort to tranfer technology across industry sectors

Most immediate perspectives for synergies (from nuclear) → Advanced high T and extreme applications

High temperature Materials:
- heat exchanger in power plants
- Gas-turbines
- Concentrated solar receivers

Materials for extreme conditions:
- Photovoltaics
- Barrier coatings
- Thermal storage
- Hydrogen
- Carbon dioxide capture

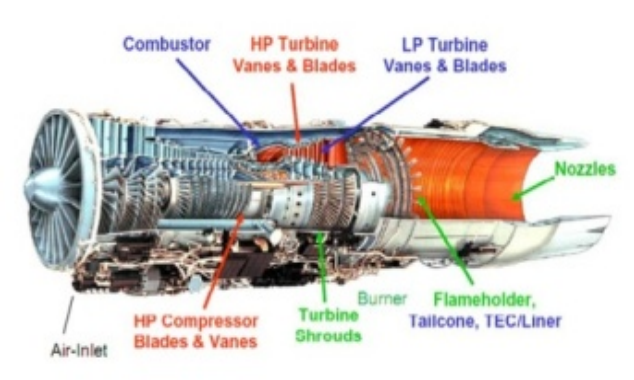

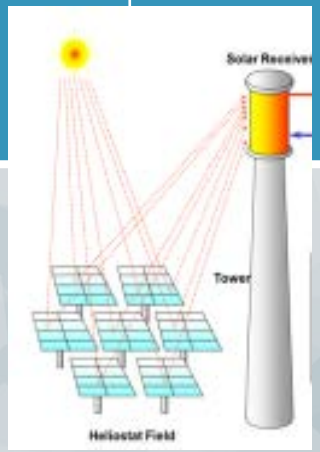

WE NEED TO INNOVATE, NOT TO INVENT : harvesting opportunity across industry

PART 1 On Ceramics for Nuclear and Concentrated Solar Power

There is an ongoing effort to tranfer technology across industry sectors

TOWER SYSTEMS suffered from insufficient “component life”, especially the receivers

The ENEA CONCEPT for next generation tower system will:

- Increase working temperature from 700 to 900 °C with new receiver
- Interfacing with high temperature thermal storage based on lead
- Interfacing with gas turbine

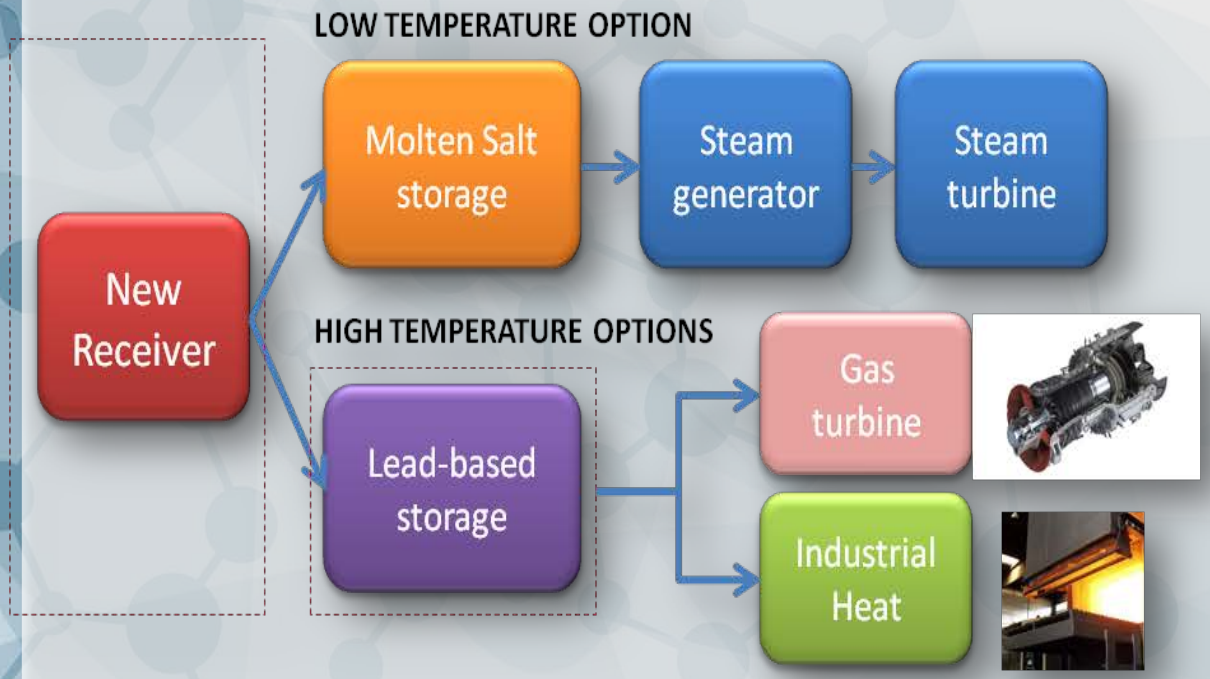

BLOCK IN NEXTOWER’s SCOPE

PART 1 On Ceramics for Nuclear and Concentrated Solar Power

There is an ongoing effort to tranfer technology across industry sectors

REQUIREMENTS OF NEW RECEIVERS

1. *Meet given thermal gradient strength*
2. *High conductivity*
3. *Manufacturing: low cost, high-throughput & high control (low defects)*
4. *Oxidation resistant*
5. *Reliable joining*
6. *Modeling and inspection/NDE*

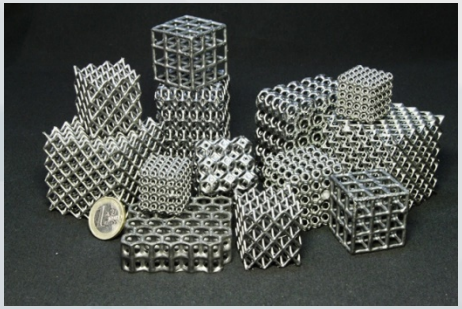

We are exploiting 2 solutions based on monolithic SiC-based, e.g. Si-SIC or All-SIC (industrial scale production)

PART 1 On Ceramics for Nuclear and Concentrated Solar Power

There is an ongoing effort to tranfer technology across industry sectors

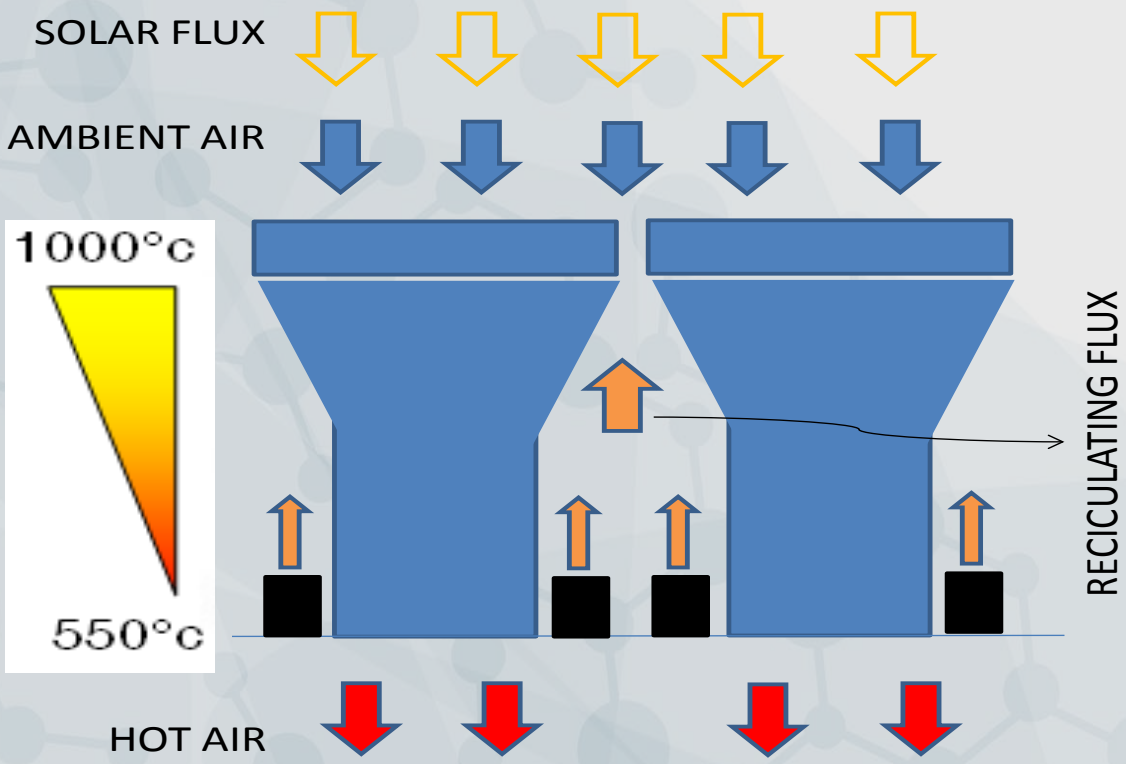

THERE ARE THERMAL GRADIENTS & THERMAL SHOCK ON MATERIALS IN THE RECEIVER

PART 1 On Ceramics for Nuclear and Concentrated Solar Power

There is an ongoing effort to tranfer technology across industry sectors

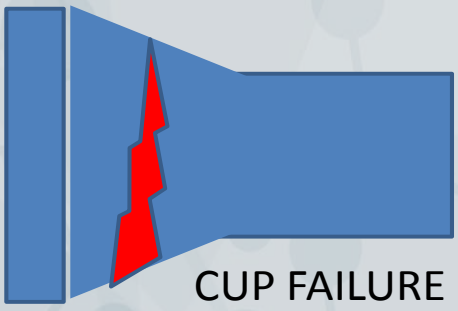

CUP FAILURE

JOINING FAILURE

1st generation CUPS made of Si-SiC and suffer from early failure:

- Fail in “intragranular” mode
- Fail at the interface between CUPS and TILES

(results from the SOLAIR FP7 PROJECT and* EU FP5 HitRec *from our sister program JP-CSP)*

1. We need materials with 99% survival probability at thermal gradient > 80°C/cm
2. **Both BULK & JOINING ARE KEY !!!!**

PART 1 On Ceramics for Nuclear and Concentrated Solar Power

There is an ongoing effort to tranfer technology across industry sectors

POSSIBILITY #1: (Si)SIC + hetero-joining

1. *High thermal conductivity due to Si phase*
2. *High toughness due to Si phase*
3. *Cheap*
4. *Could be produced from powders using additive manufacturing*
5. *Joining by many oxides*

Method	Process Condition	Material/Phase in Joint	Typical Strength
Glass-ceramic joining	1375°C, pressureless	Mullite, cristobalite, keivyite	~100 MPa
Metallic braze-based joining	~1400°C, pressureless	Si, MSi_2 (M=Ti, Cr)	~100 MPa 4PB[2] or shear
Si-C reaction bonding	~1425°C, pressureless	SiC, Si	Up to ~250 MPa 4PB
Preceramic polymer joining	1000 – 1400°C, pressureless	Si-O-C (-N)	Up to tens MPa, SLO[3] shear

PART 1 On Ceramics for Nuclear and Concentrated Solar Power

There is an ongoing effort to tranfer technology across industry sectors

POSSIBILITY #2: All SIC

1. *High thermal conductivity*
2. *High oxidation resistance*
3. *Cheap Enough*
4. *Could be produced from powders in large Q.*
5. *Joining by crystalline SiC*

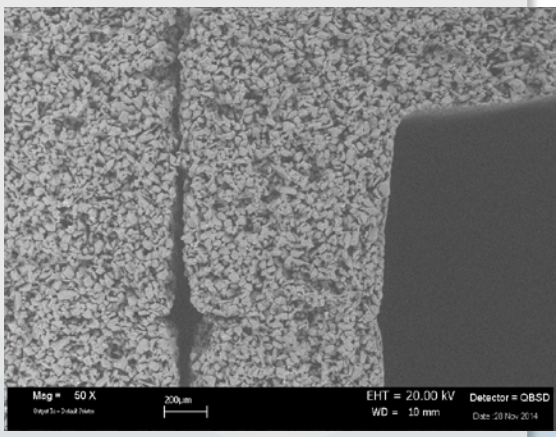

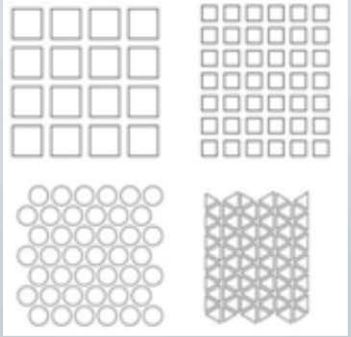

PART 1 On Ceramics for Nuclear and Concentrated Solar Power

WHY ARE WE INSISTING ON MONOLITHIC CERAMICS

ECONOMIC COMPARISON

Monolithic options (from powders):

SiSiC: <50€/Kg (conductivity/ductility) Vs. All-SiC: 50-100€/Kg (better oxidation)

Both are technically valid and economically viable

CMC (ceramic matrix composites) options (from fibers+CVI):

SiC/SiC: 5000€/Kg Tolerated thermal gradient > 120°C/cm

Effects from aeronautic booming industry? economy of scales and increased T operations may make it worthy in the future the extra performance offered by the CMC

ENPHASIS IS ON RELIABILITY AND LOW COSTS RATHER THAN A RADICAL INCREASE IN T !!!

PART 1 On Ceramics for Nuclear and Concentrated Solar Power

INDICATIONS BY THE SET-PLAN:

NEXT GEN CSP DEMANDS REDUCTION IN :

- *LOWER LEVELIZED COST OF ELECTRICITY (**LCOE**)*
- *TARGET **LCOE BELOW** **10-15 c€/kWhe*** (credit SET-PLAN)

IMPLICATIONS FOR POSSIBLE SOLUTIONS :

- *Lifetimes of the order of 20 to 25 years, with minimal down and service time*
- *Large investment may be acceptable but is a potential downside for smaller systems … CAPEX reduced by achieving economy of scale*
- Condition the choice of the ADVANCED MATERIALS we can select/design for this application
- Efficiency can be improved by a T raise only to a certain extent (e.g. emissivity losses, convection, etc.)

ENPHASIS IS ON RELIABILITY AND LOW COSTS (rather than a radical increase in T…)

Conclusions

CONCLUSIONS: we have a trajectory for deploying new high-temperature ceramic and metallic materials in CSP. For ceramics, we exploit superior properties such as :

- ✓ *High thermal conductivity → TH. GRADIENT STRENGTH*
- ✓ *High oxidation resistance*
- ✓ *Cheap and scalable , yet flexible & reliable*
- ✓ *Reliable Joining (even by crystalline SiC)*
- ✓ *Multiscale modeling/testing and NDE to support design*
- ✓ *More performing solutions offered by CMC may be at reach soon through economy of scale "leap forward" + introduction of liquid metal (e.g. liquid lead) storage options*

Thermostructural SiC based materials and composites are unfolding nicely and gaining momentum, offering opportunity for technological deployment and transfer for the nuclear community (where the market will never reach the scale of aerospace of wide spread CSP).

PART 2

In-Situ Characterization for:

- Residual Stress
- Nanoscale (sample-size) effects

PART 2 Residual Stress and In-Situ Characterization

RESIDUAL STRESSES: THE CASE OF BLISTERING IN Cu_2ZnSnS_4 (CZTS) THIN FILMS

Accepted Manuscript

Blistering in Cu_2ZnSnS_4 thin films: Correlation with residual stresses

C. Malerba, M. Valentini, C.L. Azanza Ricardo, A. Rinaldi, E. Cappelletto, P. Scardi, A. Mittiga

PII: S0264-1275(16)30910-8
DOI: doi: 10.1016/j.matdes.2016.07.019
Reference: JMADE 2023

To appear in:

Received date: 4 May 2016
Revised date: 5 July 2016
Accepted date: 6 July 2016

Please cite this article as: C. Malerba, M. Valentini, C.L. Azanza Ricardo, A. Rinaldi, E. Cappelletto, P. Scardi, A. Mittiga, Blistering in Cu_2ZnSnS_4 thin films: Correlation with residual stresses, (2016), doi: 10.1016/j.matdes.2016.07.019

PART 2 Residual Stress and In-Situ Characterization

RESIDUAL STRESSES: THE CASE OF BLISTERING IN Cu_2ZnSnS_4 (CZTS) THIN FILMS

- SEM gallery

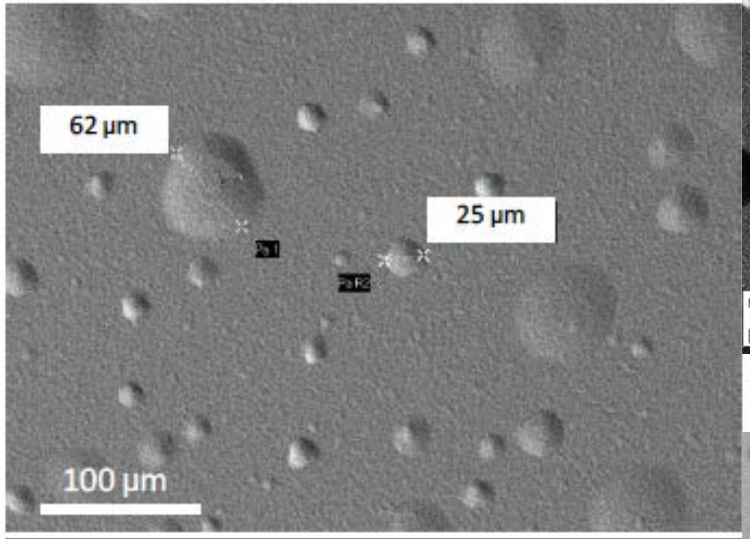

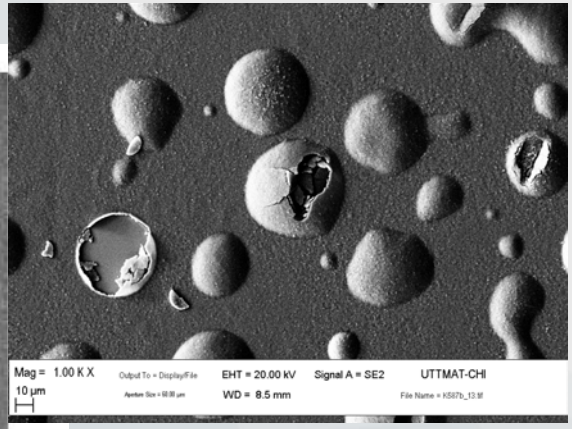

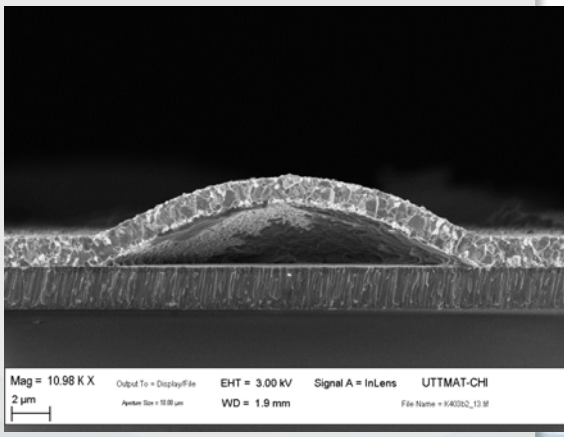

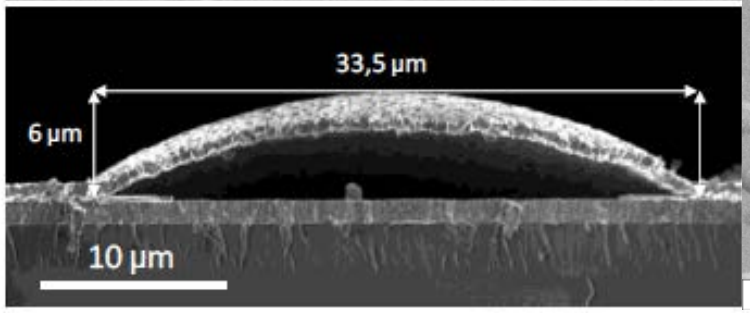

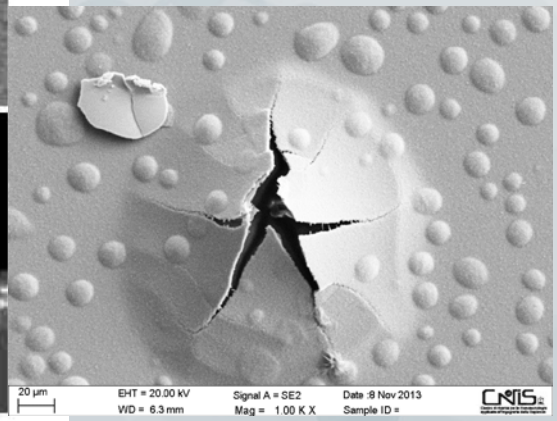

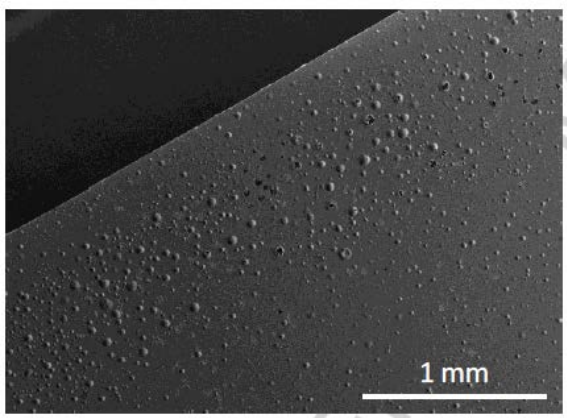

Figure 1: Typical blistering effect in CZTS film deposited on a Mo coated soda-lime glass

PART 2 Residual Stress and In-Situ Characterization

RESIDUAL STRESSES: THE CASE OF BLISTERING IN Cu_2ZnSnS_4 (CZTS) THIN FILMS

- An investigation of blistering effect in Cu_2ZnSnS_4 thin films grown by sulphurization of co-sputtered quaternary precursors is presented.
- Upon the **heat treatment at 550° C, several blisters can be often observed** in the final material. SEM cross-sections show that film delamination occurs at the CZTS/substrate interface.
- In view of CZTS application as **absorber layer in solar cells**, the formation of blisters is clearly detrimental, giving rise to shunting paths. This problem is currently the main morphological limit of our devices, which reached efficiency of 6-7% only on a small area (0.1-0.2 cm^2).
- Blistering effects have been widely reported in the literature for several materials, and was recently observed even in CZTS thin films sputtered from a quaternary target.
- Two main competing mechanisms have been suggested to explain such effect, based on relief of compressive stress or on formation of over-pressurized trapped-gas bubbles, respectively. In this work, both gas-driven and stress-driven model have been evaluated to explain blister formation in our samples.

PART 2 Residual Stress and In-Situ Characterization

RESIDUAL STRESSES: THE CASE OF BLISTERING IN Cu_2ZnSnS_4 (CZTS) THIN FILMS

CZTS thin film growth

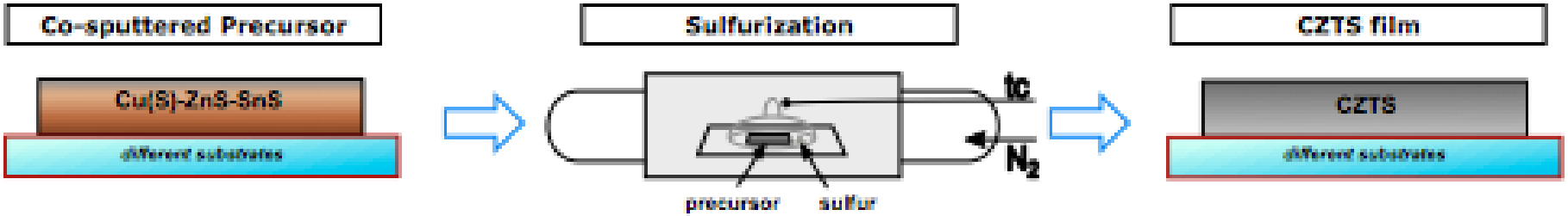

Two set of samples were deposited at different Ar pressures:

- Cosputtered from **CuS-ZnS-SnS** targets
- Cosputtered from **Cu-ZnS-SnS** targets using an additional source for sulfur vapour

- ✓ Heating ramp = 20°C/min
- ✓ T=550°C for 60 min
- ✓ Natural cooling

Sputtering powers were tuned to obtain CZTS samples with right composition (checked by EDX)

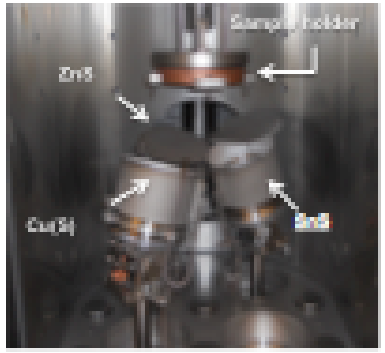

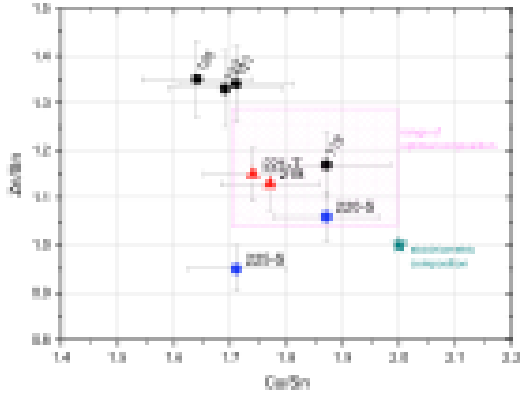

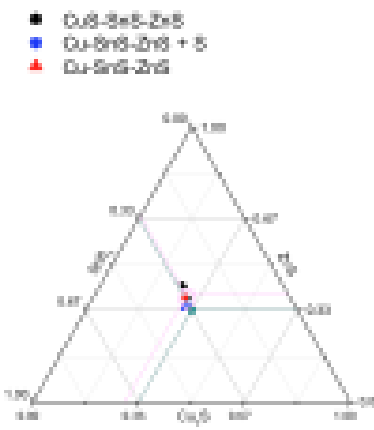

PART 2 Residual Stress and In-Situ Characterization

RESIDUAL STRESSES: THE CASE OF BLISTERING IN Cu_2ZnSnS_4 (CZTS) THIN FILMS

Measurements of substrates bending

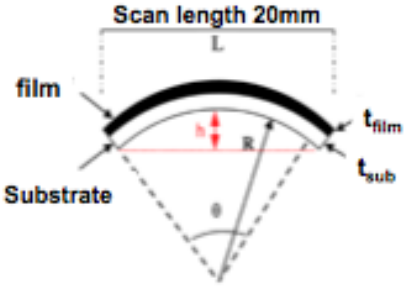

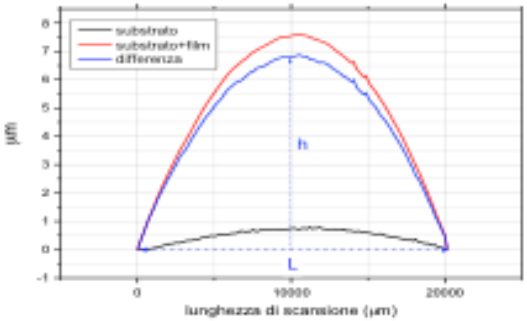

Stoney equation:

$$\sigma = \frac{E_{sub}}{6(1-\upsilon_{sub})} \cdot \frac{t_{sub}^2}{t_{film}} \cdot \frac{1}{R}$$

$$R = \frac{L^2}{8h} \quad L >> h$$

Substrate	t_{sub} (um)	E_{sub} (Gpa)	υ_{sub}
c-Si (HF)	250	169	0.3
SL-glass	150	72	0.23

Stress measurements by XRD

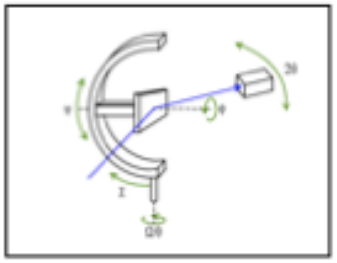

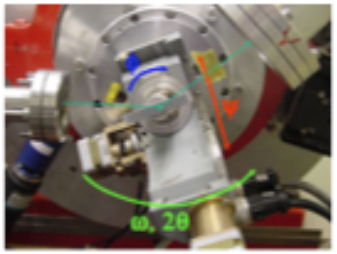

The $\sin^2\psi$ method

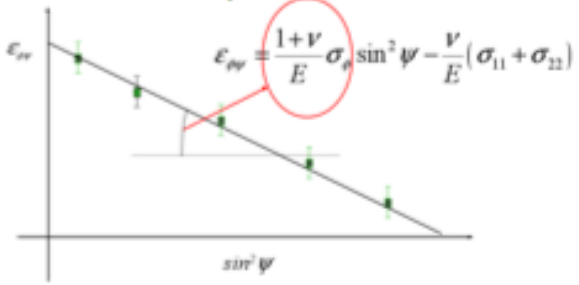

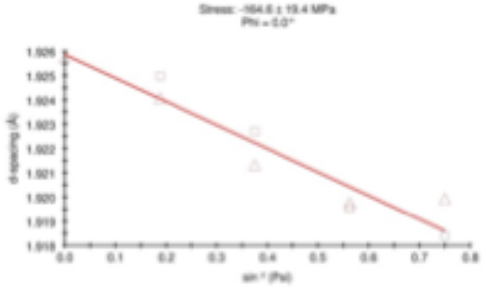

GAS DRIVEN MODEL

$$p = \left[\frac{16th\sigma}{c^2} + \frac{128\,Eth^3}{3c^4(1-\nu)}\right] = \left[\frac{16th\sigma}{c^2} + p_{\sigma=0}\right].$$

PART 2 Residual Stress and In-Situ Characterization

RESIDUAL STRESSES: THE CASE OF BLISTERING IN Cu_2ZnSnS_4 (CZTS) THIN FILMS

Residual Stresses effect on Blistering

Influence of Sputtering pressure

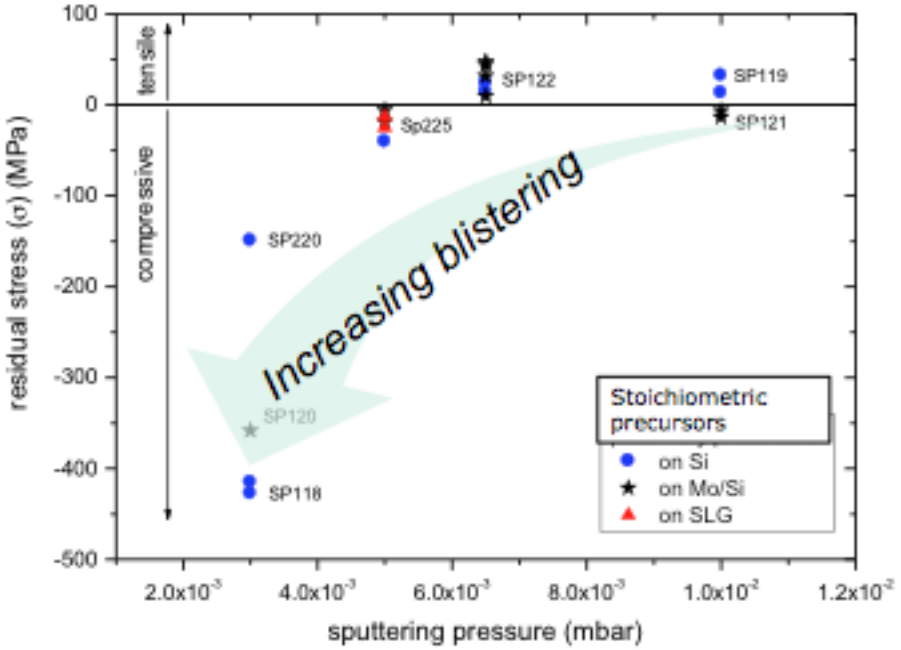

Extent of Blistering

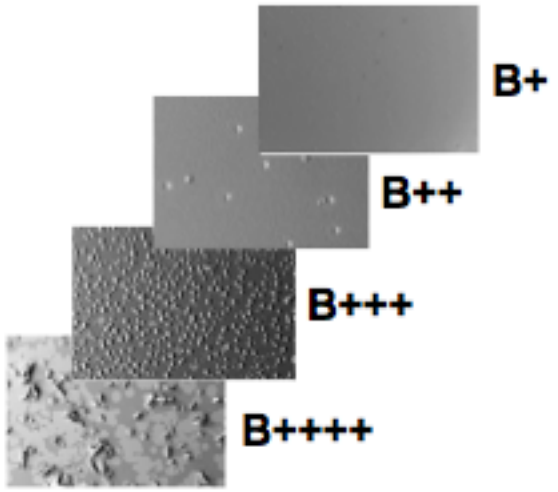

- Reduction of blistering increasing the sputtering pressure (completely removed at P > 5 10^{-3}mbar)
- A correlation between blistering extent and residual stress of precursors is observed
- Residual stress of precursors is independent of substrate
- No signal of sputtering gas (Ar) detected by EDX (even at the lowest pressure)

PART 2 Residual Stress and In-Situ Characterization

RESIDUAL STRESSES: THE CASE OF BLISTERING IN Cu_2ZnSnS_4 (CZTS) THIN FILMS

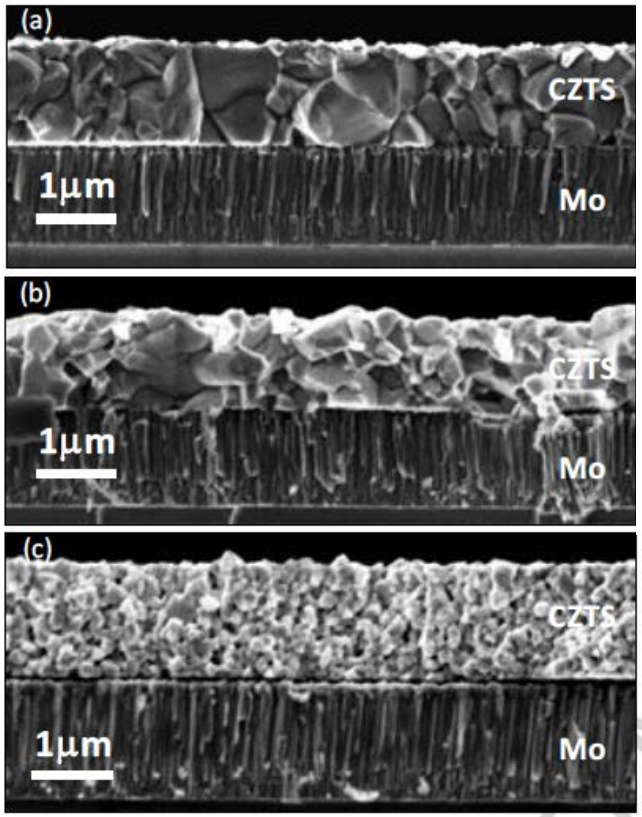

Figure 10: Cross-sectional SEM images of CZTS samples on SLG/Mo substrates obtained from precursors deposited at different sputtering pressures: a) K611b – SP220 ($3 \cdot 10^{-3}$mbar); b) K614b – SP225 ($5 \cdot 10^{-3}$mbar); c) K615b – SP229 ($6.5 \cdot 10^{-3}$mbar).

Prec.#	T °C	P(Ar) mbar	d_{SP} nm	σ_{SP} MPa	Kest.#	d_{Kest} nm	K/Si	K/Mo/Si	K/SLG	K/Mo/SLG
Type A:	*CuS-SnS-ZnS*									
SP118	amb	$3 \cdot 10^{-3}$	800	-300	K535	840	B+	B	/	B-
SP122	amb	$6.5 \cdot 10^{-3}$	1030	+20	K537	1050	NB	NB	NB	NB
SP119	amb	10^{-2}	760	+5	K536	800	NB	NB	/	NB
Type B:	*Cu-SnS-ZnS +S*									
SP220	150	$3 \cdot 10^{-3}$	1300	-120	K611	1270	B+++	/	B+++	B+
SP225	150	$5 \cdot 10^{-3}$	1270	-20	K614	1240	B	/	B	NB
SP229	150	$6.5 \cdot 10^{-3}$	1200	+25	K615	1170	NB	/	NB	NB

Table 1: List of sputtered-precursors, with corresponding deposition conditions (substrate temperature, T, and sputtering pressure, P), thickness (d_{SP}) and average residual stress from curvature measurements (σ_{SP}). The corresponding kesterite samples (converted precursors), with final thickness d_{kest}, are also reported, together with the extent of blistering (from NB to B+++) observed on different substrates (Si, Si/Mo, SLG, SLG/Mo).

PART 2 Residual Stress and In-Situ Characterization

RESIDUAL STRESSES: THE CASE OF BLISTERING IN Cu_2ZnSnS_4 (CZTS) THIN FILMS

XRSA: X-Ray Stress Analysis

With this technique, a biaxial (in-plane) residual stress is obtained from a plot of the interplanar distance (dhkl) along a given [hkl] crystallographic direction versus sin2ψ , wherethe ψ– tilt is the angle between the normal to the thin film surface and the diffraction plane
(HP: planar and equibiaxial stress)

Table 3: XRSA results (in MPa) for samples SP220, SP225 and SP229 on SLG. See text for details.

		Constant stress	Linear stress trend		
			AVE	Surf	Interface
SP220	Reuss	-90	-130	10	-270
	Hill	-120	-180	15	-380
	Meas	-115	-168	25	-370
SP225	Reuss	-20	-38	20	-100
	Hill	-30	-50	20	-125
	Meas	-29	-48	30	-130
SP229	Reuss	45	50	40	70
	Hill	60	68	40	100
	Meas	57	64	40	90

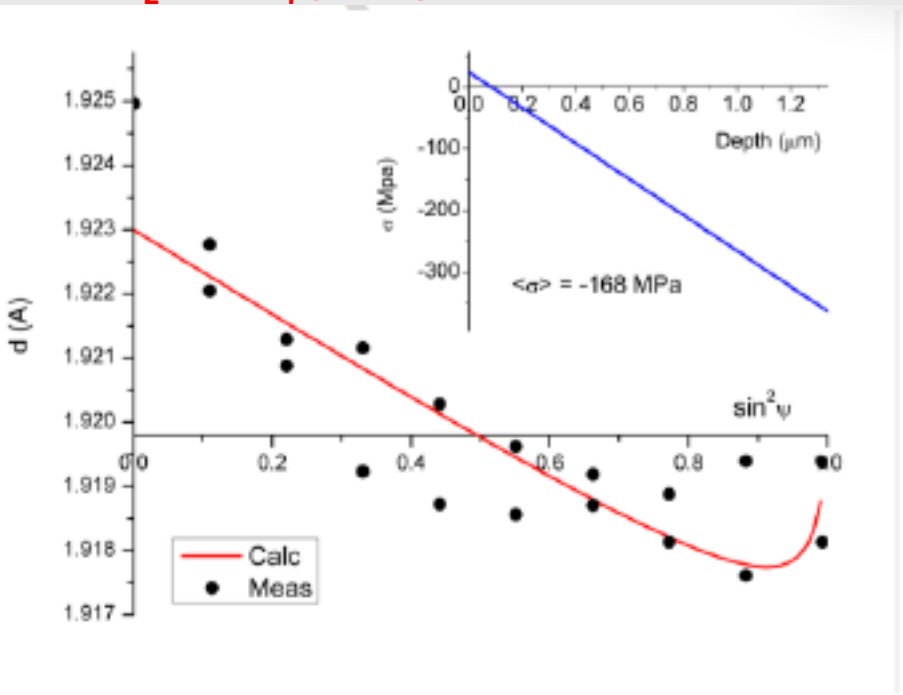

Figure 6: $Sin^2\psi$ plot (interplanar distance *d* as a function of squared sine of ψ-tilt angle) assuming a linear stress trend (sample SP220/SLG, [220] peak). The inset shows the stress variation across the film thickness (0 at the surface).

$$|\sigma| = 4.88 \frac{E_{film}}{1-\nu_{film}^2}\left[k\left(\frac{h}{c}\right)^2 + \left(\frac{t_{film}}{c}\right)^2\right]$$

PART 2 Residual Stress and In-Situ Characterization

RESIDUAL STRESSES: THE CASE OF BLISTERING IN Cu_2ZnSnS_4 (CZTS) THIN FILMS

Instrumented nanoindentation tests (InSEM,Nanomechanics Inc., USA) were conducted by using a three-sided Berkovich diamond tip, for the purpose of assessing the mechanical properties of the deposited CZTS and provide an experimental input value of the Young's modulus ECZTS to be used in XRSA.

Experimentally measured value of ECZTS = 55 GPa for Young's modulus is used).

This model is not compatible with the experimental evidence, as it predicts stress values much higher than the measured ones, which in most cases are below 100 MPa.

NB reference CZTS value for Young's modulus is 78 GPa

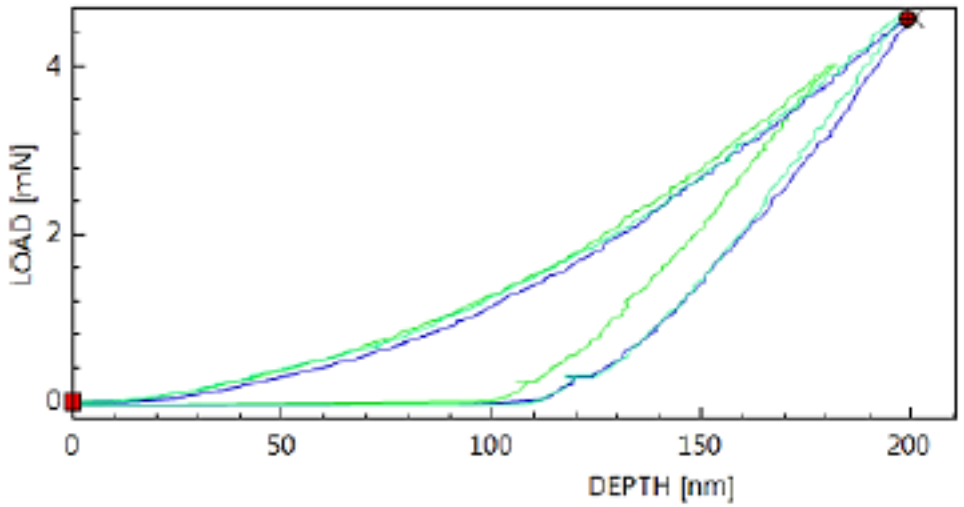

Figure 7: Load – depth curve from nanoindentation measurements in three different points of SP220.

$$E_{CZTS} = \left(\frac{1}{E^*} - \frac{1-\nu_{TIP}^2}{E_{TIP}}\right)^{-1}(1-\nu_{CZTS}^2)$$

PART 2 Residual Stress and In-Situ Characterization

RESIDUAL STRESSES: THE CASE OF BLISTERING IN Cu_2ZnSnS_4 (CZTS) THIN FILMS

The model could be improved by considering that the observed blister formation is likely related both to rate-dependent and to rate-independent plastic deformation of the film at the temperature of heat-treatment. Indeed, the sulfurization temperature (823 K) is >65% of Tmelt (CZTS) (1253 K), well above the typical threshold for the emergence of creep deformation processes (typically 40-50% of Tmelt)

A simple confirmation of this hypothesis is that the fragments of broken blisters (Figure 12b) retain the

Under the hypothesis of viscoplastic material, the driving force necessary for blistering (compressive stress or gas pressure in this case) is well below the limit predicted in the elastic regime.

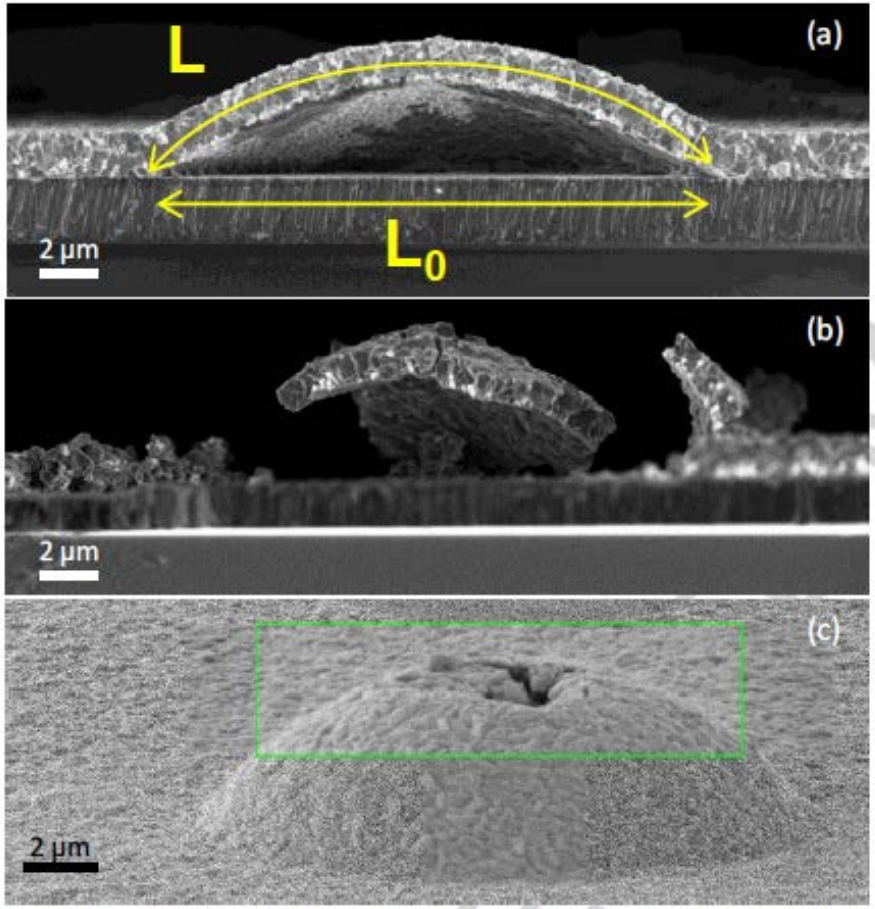

Figure 12: Typical section of a blister showing the large bending effect, together with the permanent curvature of blister fragments in vacuum at room temperature.

PART 2 Residual Stress and In-Situ Characterization

RESIDUAL STRESSES: THE CASE OF BLISTERING IN Cu_2ZnSnS_4 (CZTS) THIN FILMS

Therefore, the gas-pressure necessary to produce the same effect of a compressive
stress of -200MPa (i.e. the estimated yield stress value) would be 36 MPa. Despite this
value is well below the value predicted under elastic regime, is still higher than the gaspressure expected in our films (at least in the case of samples with the highest extent of blistering), thus suggesting that Ar trapping can only play a secondary role in blister formation

A detailed analysis of residual stresses, both by substrate-curvature and XRD methods, and of the mechanical properties by SEM-monitored nanoindentation, showed the importance of the compressive stress in the precursors in blister formation upon heat treatment. A stress-driven mechanism in viscoplastic deformation conditions has been proposed to explain the observed blistering in CZTS films, while it is observed that Ar entrapment could only contribute as a secondary effect.

CONCLUSIONS

- Blistering is a problem for the reliability of CZTS thin films grown by sulfurization of cosputtered quaternary precursors with the formation of blisters with diameters ranging between 1060 um and heights between 310 um.

- A nanoindentation study, coupled to other characterization techniques and residual stress measurements, was performed to gain greater insight and point out the role of increasing sputtering pressure on the limitation of both compressive stress in precursors and blistering extent in the corresponding CZTS film decrease.

- The direct measurements of the nanomechanical properties of assputtered CZTS indicate that stress-driven viscoplastic deformation seems the main mechanism of blistering in CZTS, while trapped Ar pressure may play just a secondary role.

PART 2 Residual Stress and In-Situ Characterization

RESIDUAL STRESSES: THE CASE OF BLISTERING IN Cu_2ZnSnS_4 (CZTS) THIN FILMS

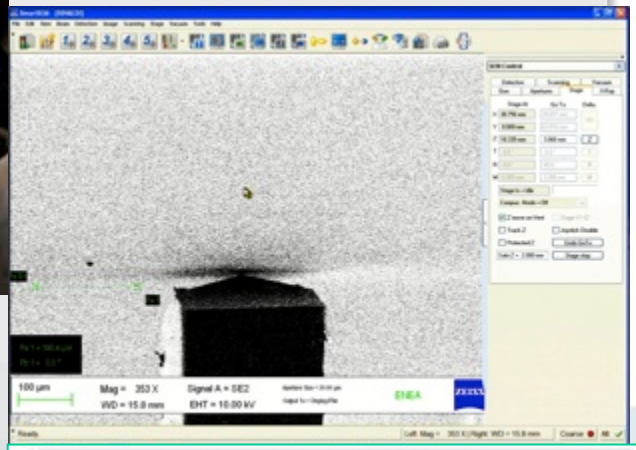

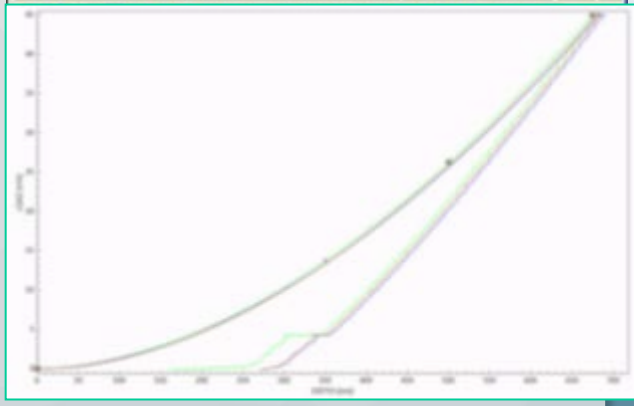

New nanoindentation facility for ex-situ and In situ Nanoindentation (here shown on our FEG-SEM also equiped with EDS and STEM)

3

2

PART 2 Residual Stress and In-Situ Characterization

IN-SITU TESTING Sometimes it is not easy to test in a random place of the surface….

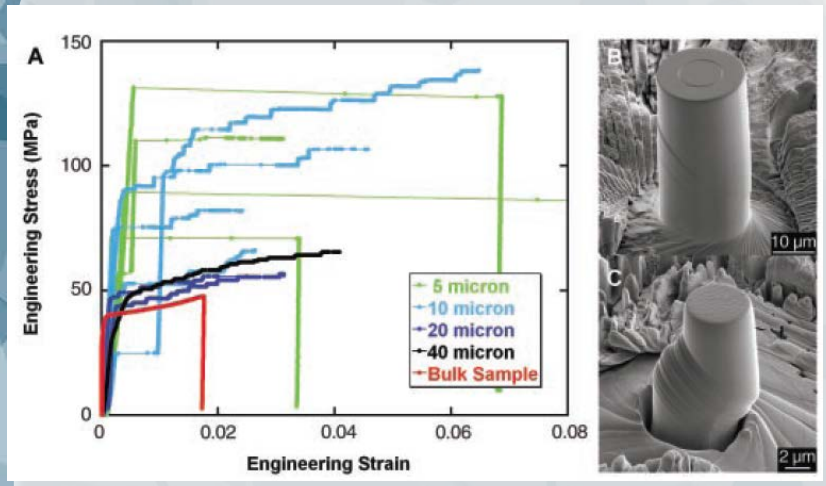

Uchic et al. Science, 305, (2004), pp. 986-989

PILLARS TESTING

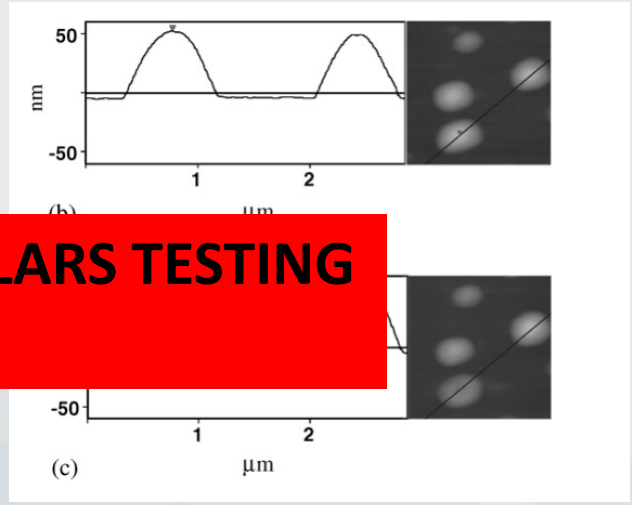

Gerberich, et al. JMPS, 51 (2003) 979 – 992

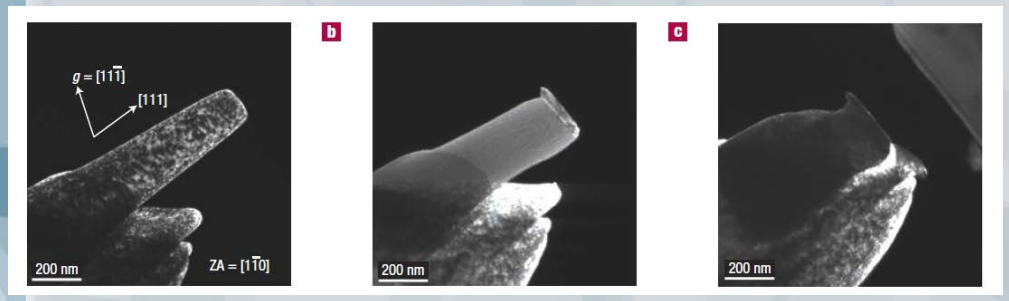

Shan et al. Nat Mat 7(2008)

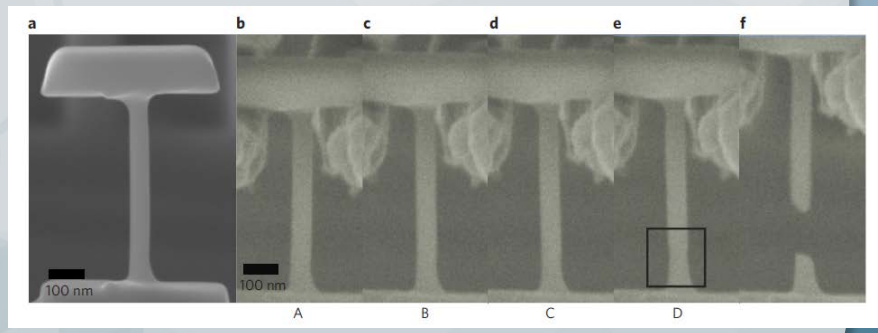

Jang et al. Nat Mat, **9**, 215-219 (2010)

PART 2 Residual Stress and In-Situ Characterization

IN-SITU TESTING

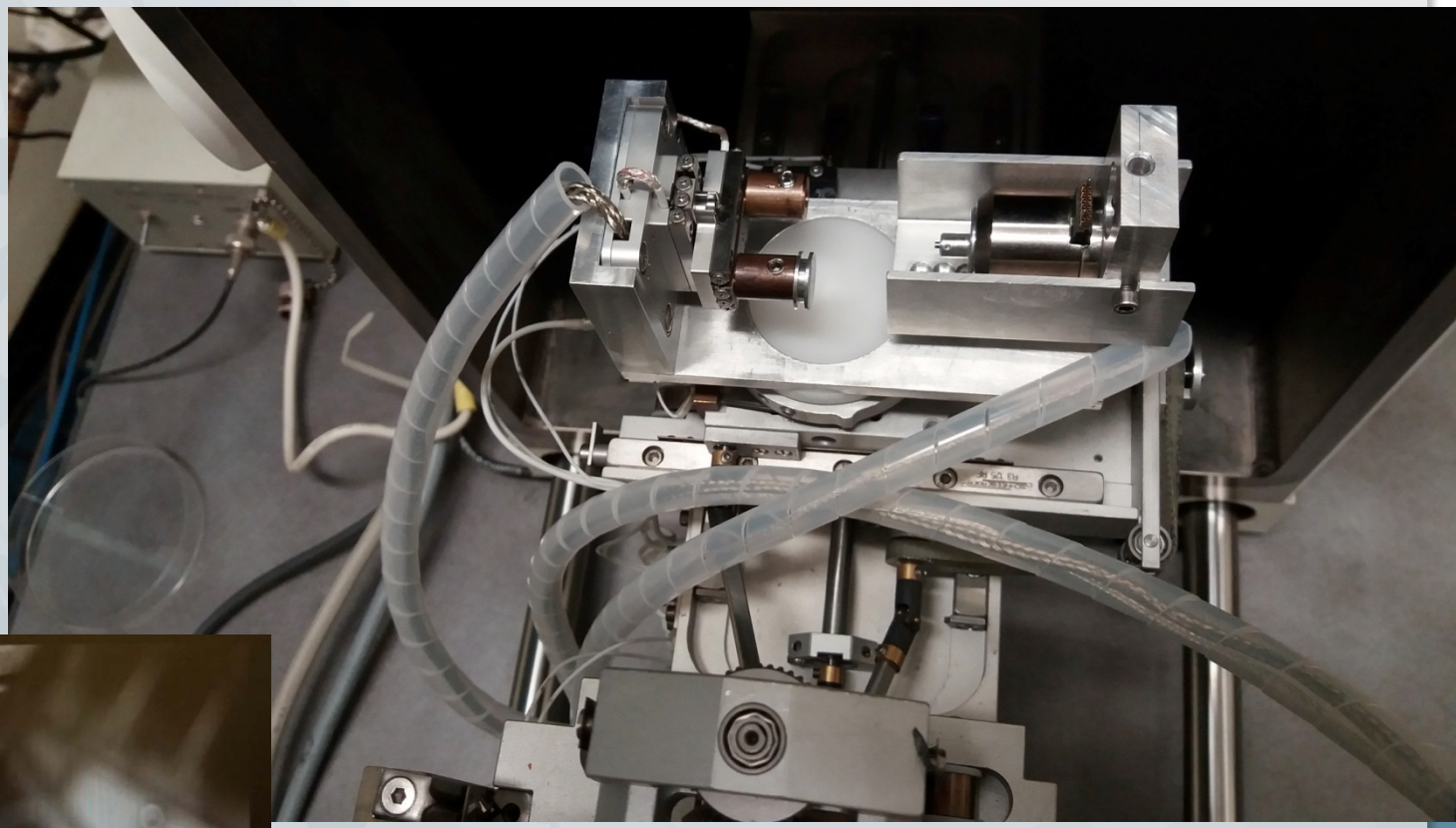

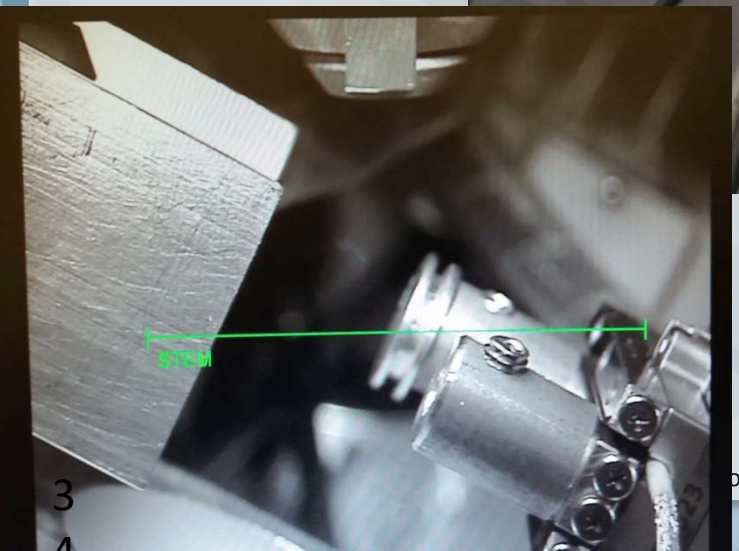

PART 2 Residual Stress and In-Situ Characterization

The sample-size effect is a STRUCTURE-PROPERTY ISSUE and the ORIGIN of this dependence in nanoscale metal pillars remains UNKNOWN

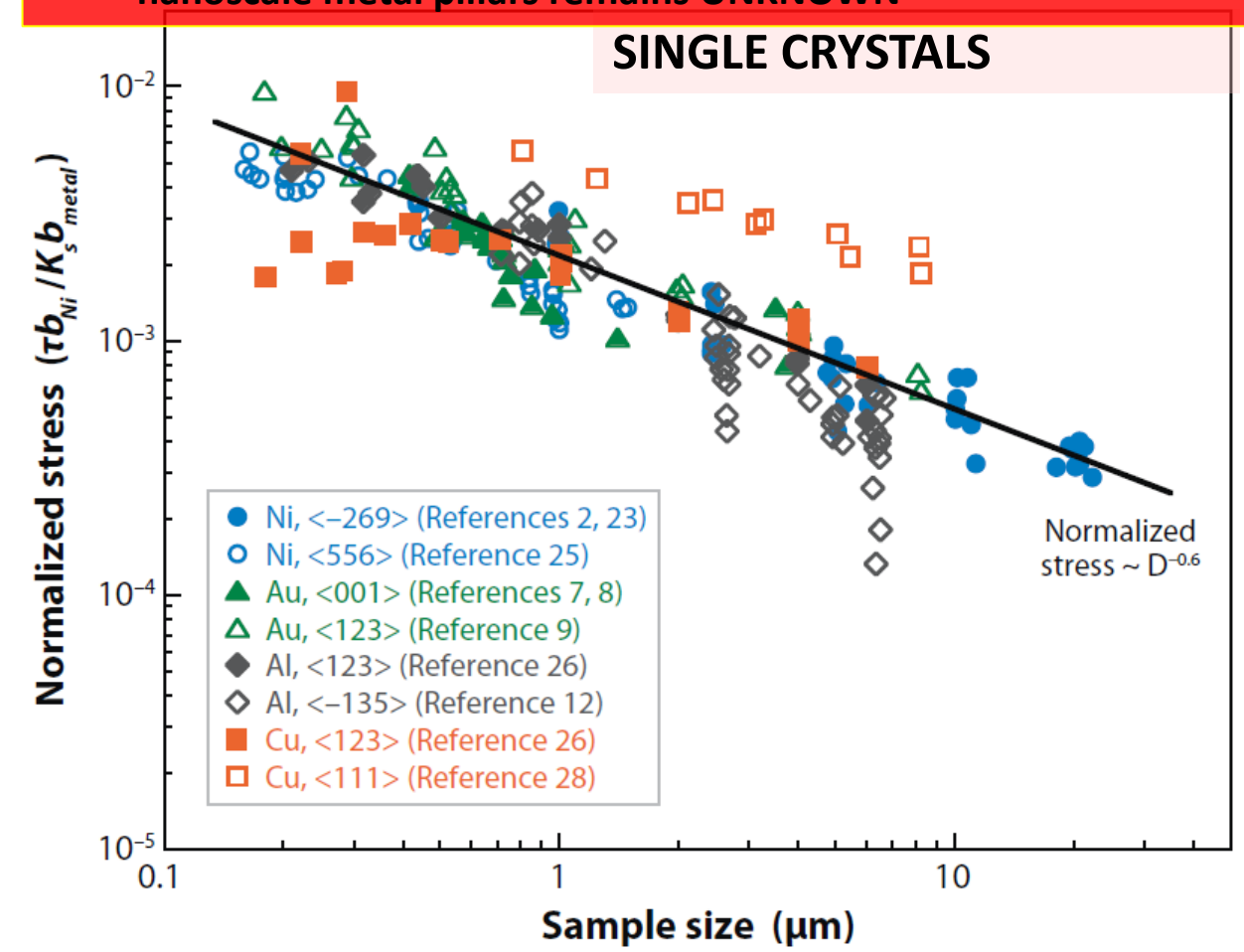

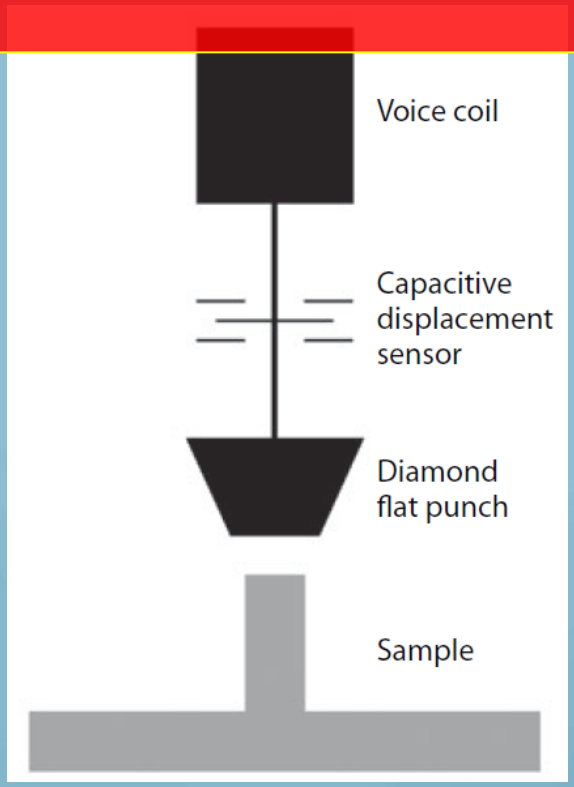

Uchic et al., Annu. Rev. Mater. Res., 2009, 39, 361–386.

Plastic strength (i.e. elastic limit) scales as power-law $\sigma_y \sim D^{-\beta}$ *(β~0.6 ?)*

→ **the smaller the stronger…**

PART 2 Residual Stress and In-Situ Characterization

IN-SITU TESTING

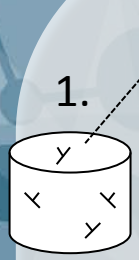

1. The root cause was first supposed to be the defect-free nature of small scale material samples, but TEM studies eventually proved pillars as small as 200 nm in diameter to be disordered systems with substantial dislocation densities ρ (e.g. $\rho \sim 10^{8\text{-}9}\ cm^{-2}$)

2. Furthermore, other defects stably residing in pillars results from FIB damage at the pillar surface (i.e. Ga atoms implantation and residual stresses)

→ two SOURCES of defects are notable theoretical complication

Yet some studies seem to point towards **bulk defects** as the most influential defects (Jennings, et al. *PRL* **104**, 135503 (2010)).

Based on that :

Let's analyze very small nanotargets to demonstrate that sample-size dependence may be intrinsically understood as a statistical fact

PART 2 Residual Stress and In-Situ Characterization

IN-SITU TESTING

HYPOTHESIS :

Pillar volume defines the probability of sampling a certain distribution of dislocations in the pillar after FIB milling.
("*inheritance*" of native dislocation density is also assumed)

1) ORDERED MATERIAL

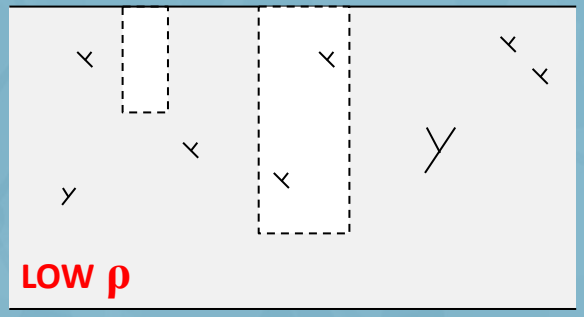

FIB MILLING

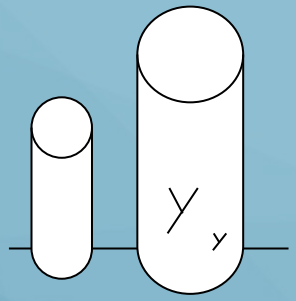

STATISTICALLY DIFFERENT

SIZE EFFECT

2) DISORDERED MATERIAL

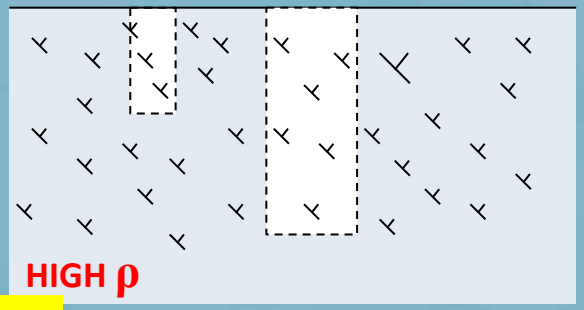

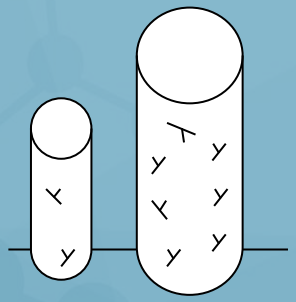

STATISTICALLY INDIFFERENT

NO SIZE EFFECT

conventional plasticity

THESIS :

If a size-dependence exists, then pillars of different size are statistically different (in dislocation content) and a Weibull argument can be drawn

PART 2 Residual Stress and In-Situ Characterization

IN-SITU TESTING

EXPERIMENTALLY:

CONTROLLING ρ

Commercial Nickel sheet, and applied cycles of thermal annealing (*remove dislocations)* and surface polishing *(introduce dislocations)*

LOW ρ

HIGH ρ

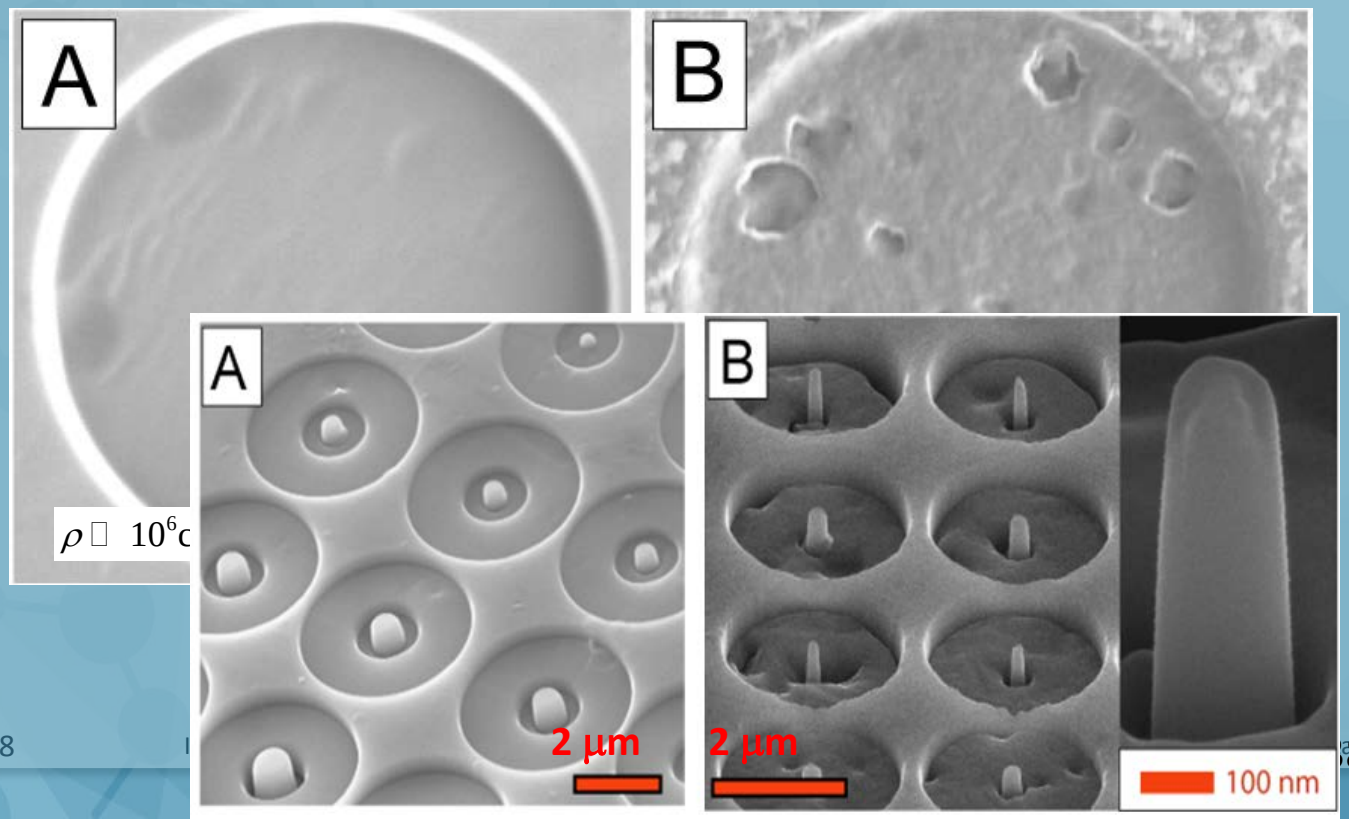

EBSD map

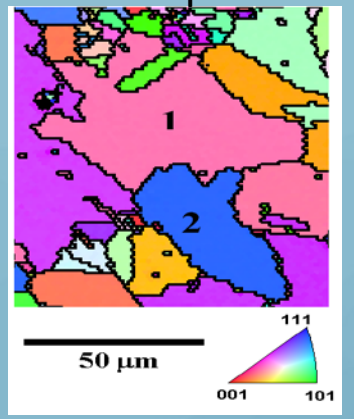

SCHMID FACTOR
0.46-0.48

Inheritance of native ρ !!

PART 2 Residual Stress and In-Situ Characterization

IN-SITU TESTING

EXPERIMENTALLY:

Rinaldi, et al. "Dislocation Density on Sample-Size Dependent Plasticity in Nanoscale Pillars and Buttons". Journal of Nanomechanics and Micromechanics, 2(3), 42-48 (2012)

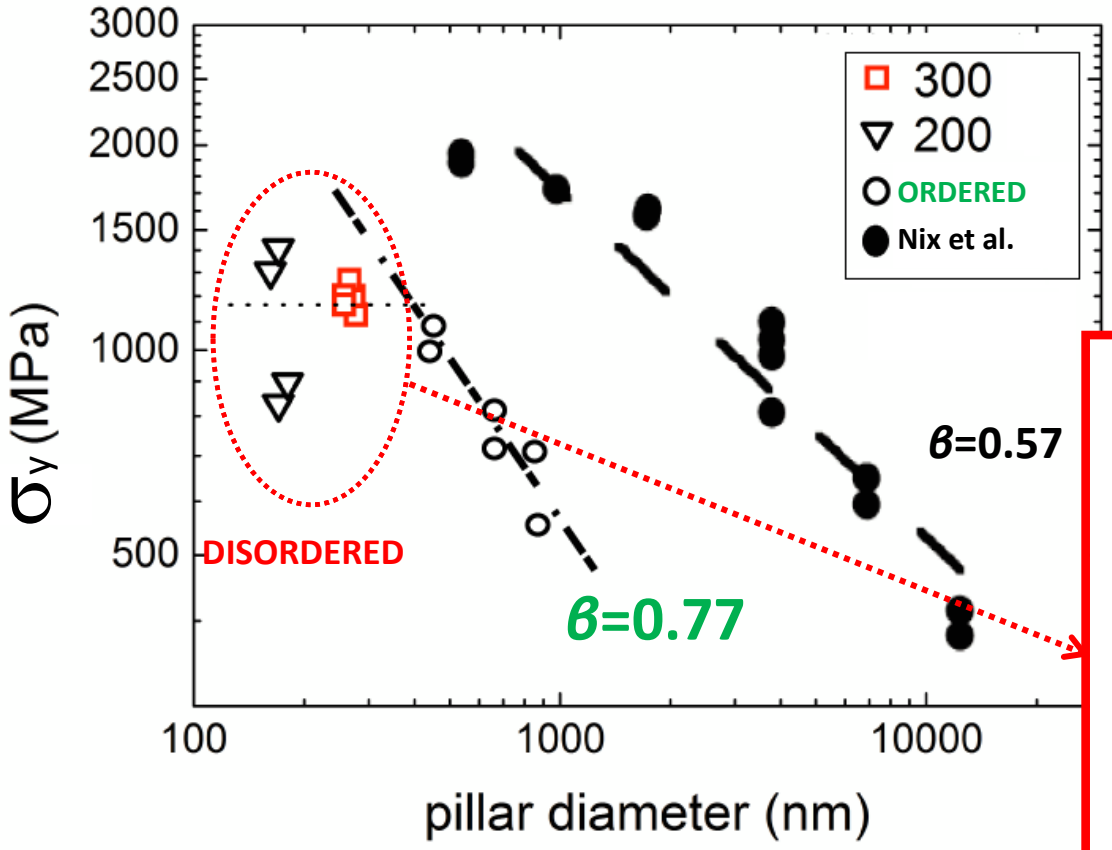

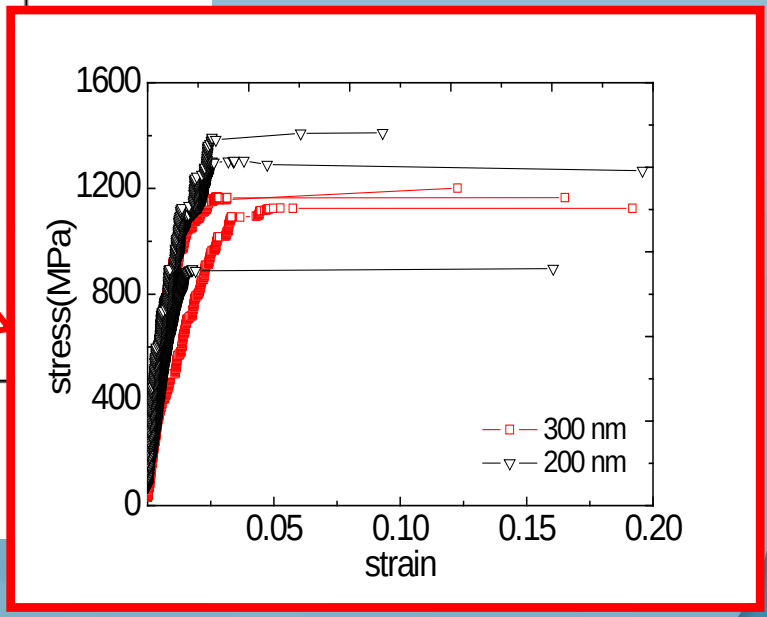

LOW ρ → yes, scaling (β=0.77)

HIGH ρ → no scaling

DISORDERED MATERIAL

PART 2 Residual Stress and In-Situ Characterization

IN-SITU TESTING

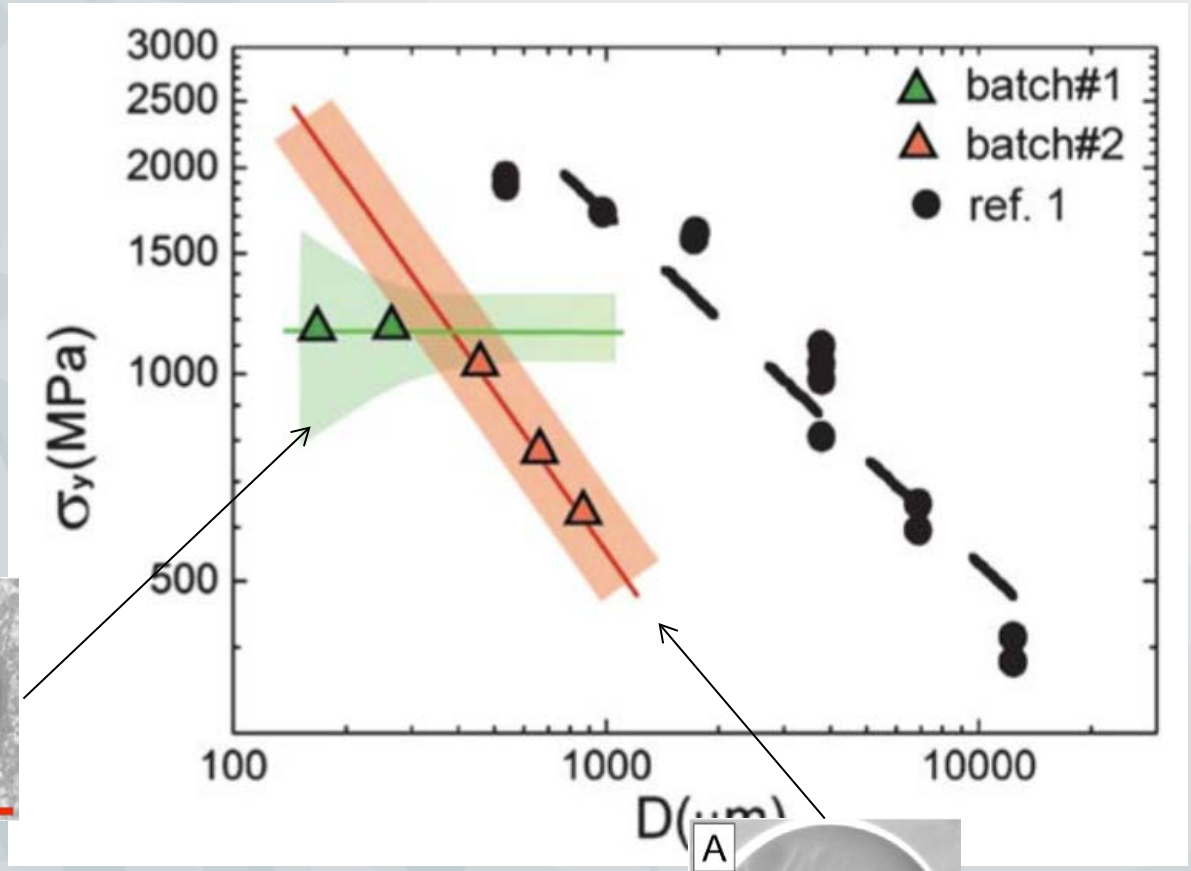

PART 2 Residual Stress and In-Situ Characterization

IN-SITU TESTING

EXPERIMENTALLY:

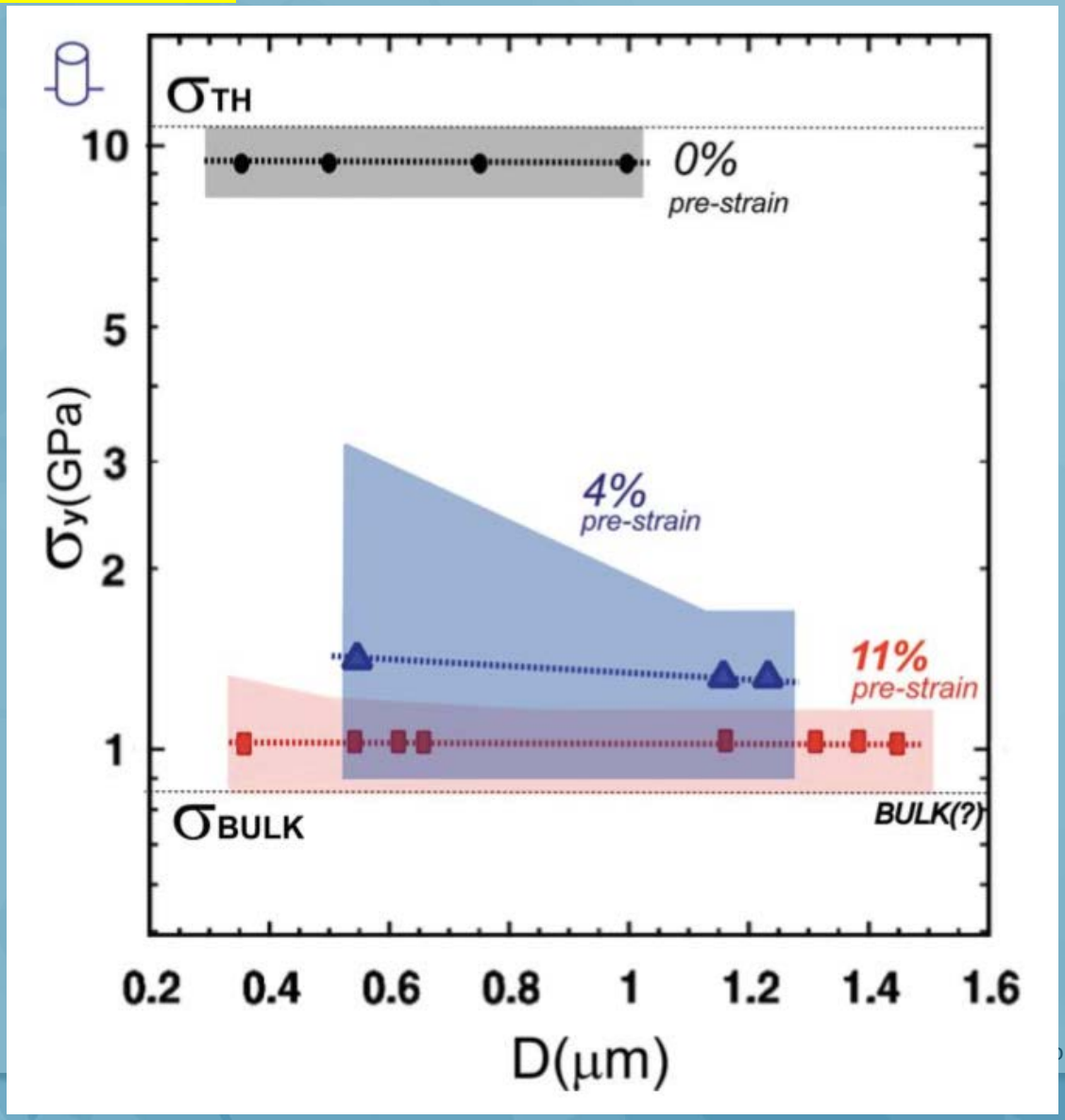

Mo-alloy pillars

H. Bei, S. Shim, G. M. Pharr and E. P. George, Acta Mater., 2008, 56, 4762–4770.

PART 2 Residual Stress and In-Situ Characterization

IN-SITU TESTING

EXPERIMENTALLY:

SEM of compressed pillars failing by Single Slip

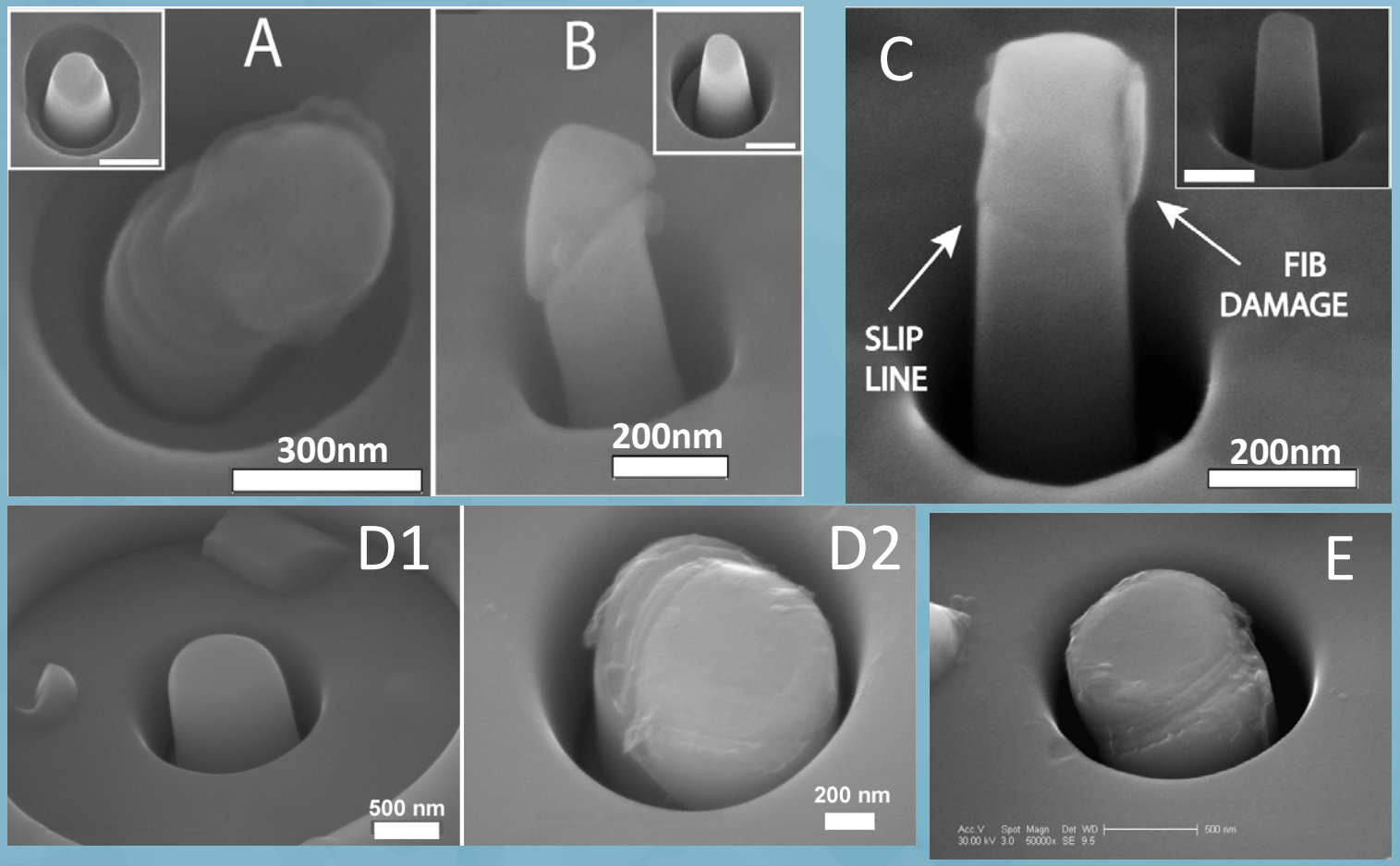

D~200 nm

D > 400nm

ALL PILLARS FAILED BY SINGLE SLIP AS EXPECTED

(several slip lines along the planes with maximum Schmid factor are well visible)

PART 2 Residual Stress and In-Situ Characterization

STATISTICAL MODELING: A PROPOSAL

Since difference in dislocation density of pillars determine the power-law, the effect at LOW ρ is VOLUME controlled in a WEIBULL sense (like for brittle materials)

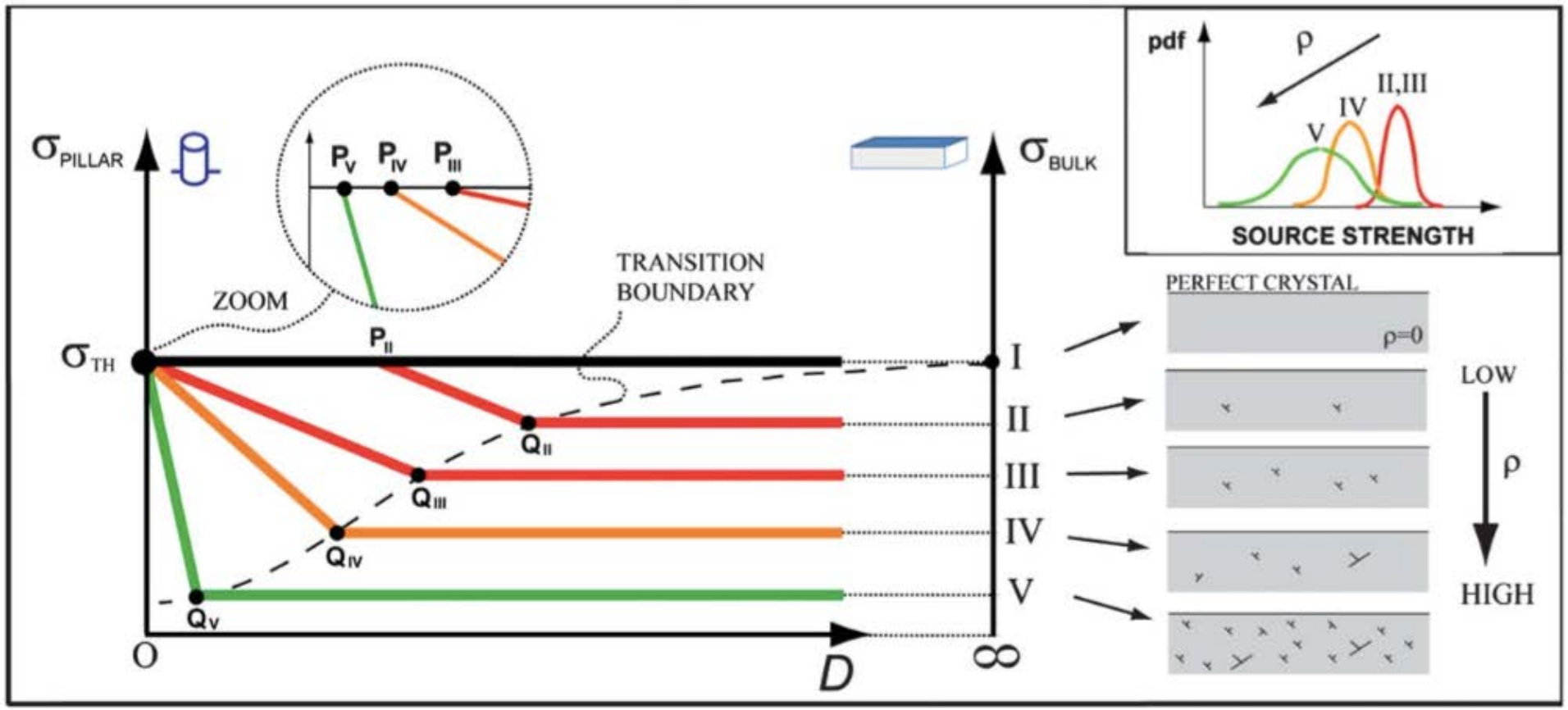

Effects of dislocation density and sample-size on plastic yielding at the nanoscale: a Weibull-like framework

Antonio Rinaldi*abc

xtreme Conditions, Sardinia, Italy, 15 to 17 May 2017

Cite this: *Nanoscale*, 2011, **3**, 4817

PART 2 Residual Stress and In-Situ Characterization

STATISTICAL MODELING: A PROPOSAL

Since difference in dislocation density of pillars determine the power-law, the effect at LOW ρ is VOLUME controlled in a WEIBULL sense (like for brittle materials)

$$F(\sigma; V) = 1 - e^{-V\left(\frac{\sigma}{\sigma_0}\right)^m} \rightarrow F(\sigma;V) = F(\sigma_{REF};V_{REF}) \rightarrow \frac{\sigma}{\sigma_{REF}} = \left(\frac{V_{REF}}{V}\right)^{1/m} \rightarrow \log \sigma \propto -\frac{3}{m}\log D$$

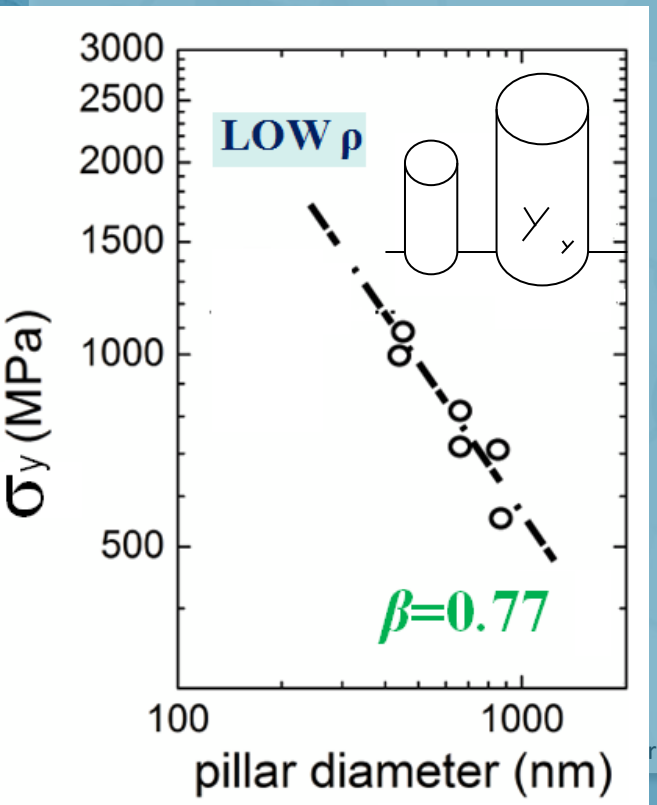

PLEASE NOTE:

- ***A SIMPLE STATISTICAL IDEA (perhaps just as a starting point)***
- ***A MANNER TO CHARACTERIZE MATERIAL DISORDER FROM NANOMECHANICS TESTS (validation work to be undertaken)***

$$m = \frac{3}{\beta}$$

m=3.9

Rinaldi, et al., *Acta Mater.*, **56**, 511 (2008)

Rinaldi, et al., *Nanoscale* DOI: 10.1039/c0nr00699h

PART 2 Residual Stress and In-Situ Characterization

IN-SITU TESTING

….. some of other related work on pillars testing from our group

NANOCRYSTALLINE Ni (20nm grains)

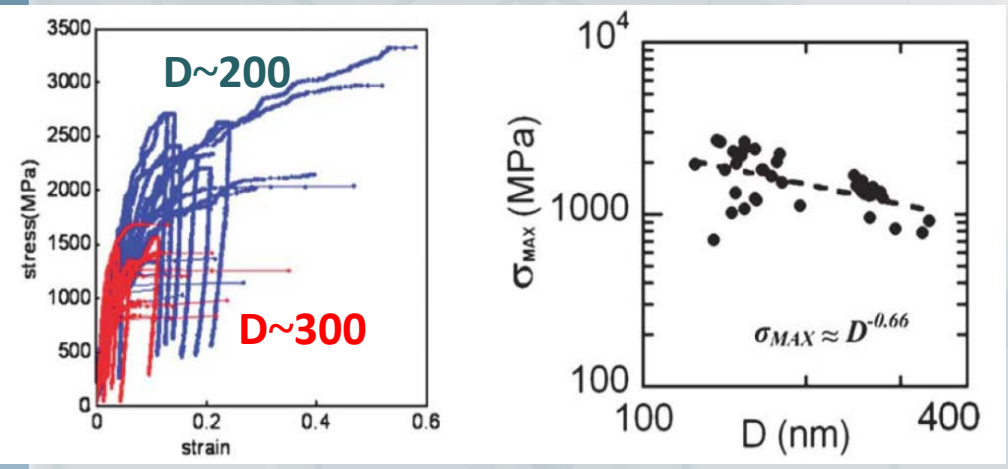

Rinaldi, et al., *Acta Mater.*, **56**, 511 (2008)

HIGH-THROUGHPUT EXPERIMENTS ON PATTERNED SURFACES

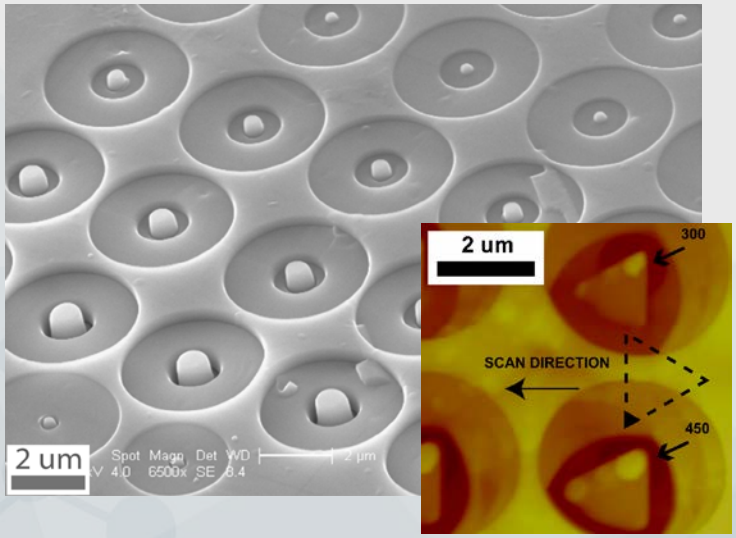

Rinaldi, et al. *J. Mater. Res.* **24**, 3, (2009)

PART 2 Residual Stress and In-Situ Characterization

IN-SITU TESTING……. Those size effects hold for CERAMICS AS WELL

Zinc-Oxide Nanopillar After controlled compression test, demostrating ductility of nanoscale ZnO

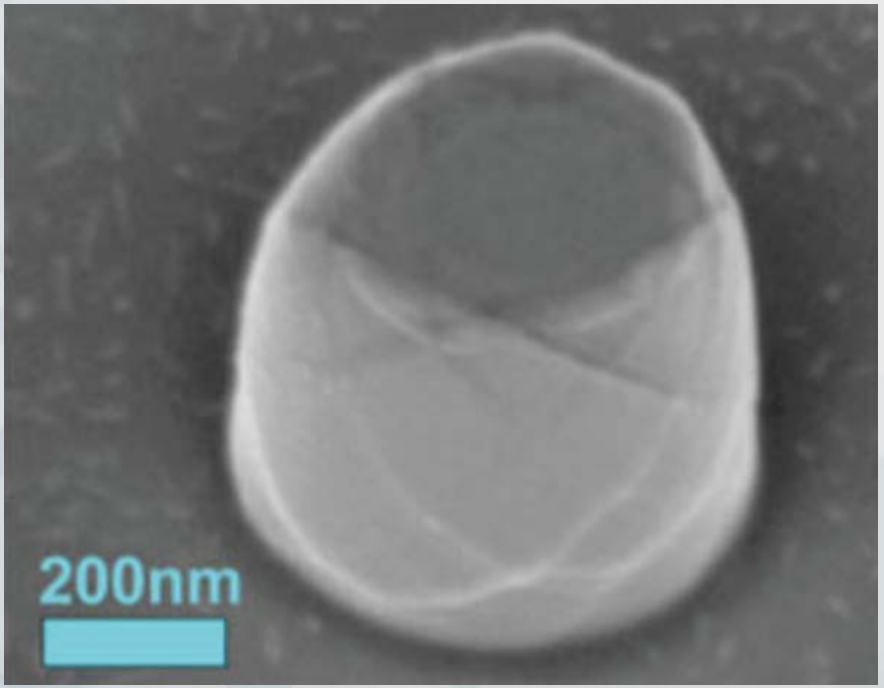

Rinaldi et al. Adv. Mater. **2014**,

PART 2 Residual Stress and In-Situ Characterization

IN-SITU TESTING

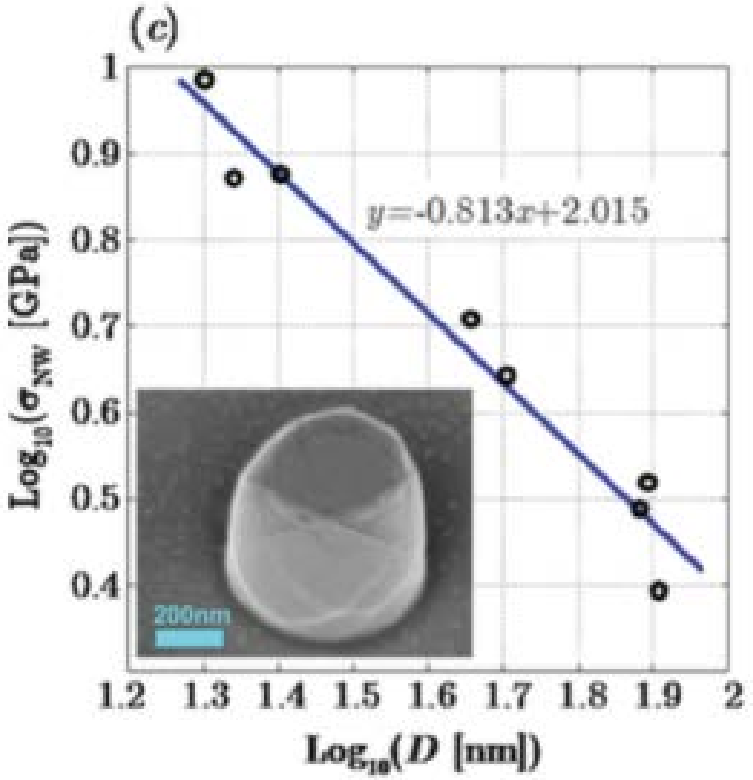

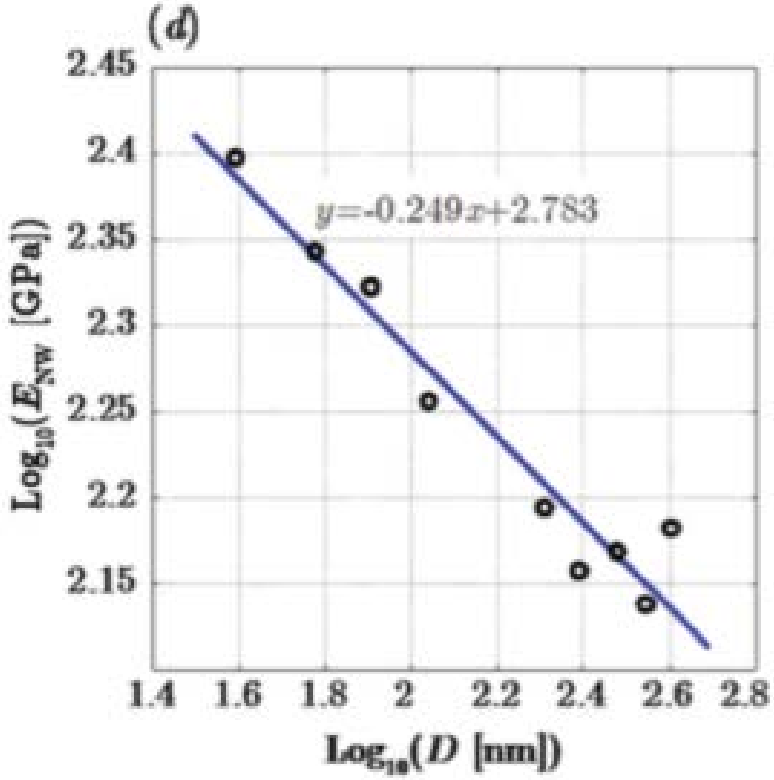

Parameter	Fracture strength	Young's modulus
R-squared:	0.960	0.941
Root mean square error:	0.046	0.024
Pearson's correlation coefficient (P-Value):	0.980	0.970

Rinaldi et al. Adv. Mater. **2014**,

PART 2 Residual Stress and In-Situ Characterization

IN-SITU TESTING: THE CASE ON ZnO NWs

The interest in ZnO has increased drastically with respect to other materials of the same wurtzite family, such as GaN, InN, and CdS, because it is an attractive low-cost II-VI semiconductive material that has a wide range of outstanding functional properties that depend on doping, including semiconductivity, piezoelectricity, pyroelectricity, direct wide bandgap (3,4 eV) with native *n*-type, high transparency, biocompatibility, excellent chemical and thermal stability, large exciton binding energy (60 meV), and room-temperature ferromagnetism.

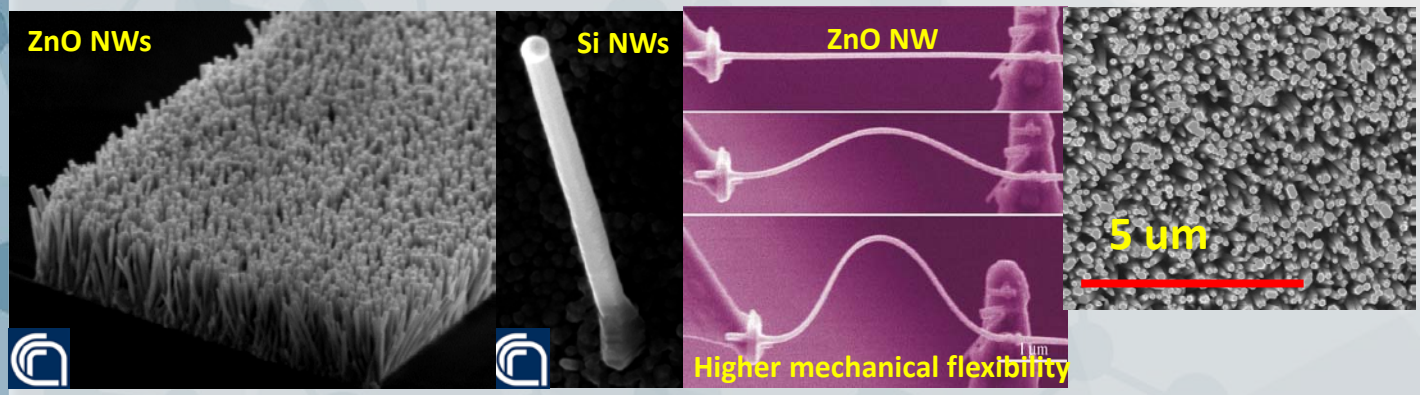

ZnO can be grown in many different nanoscale forms (it has probably the richest variety of different nanostructures) without much effort and through various swell-established methods such as vapor-liquid-solid (VLS), electrodeposition, hydrothermal growth (HTG), focused ion beam (FIB) machining, and sol-gel process.

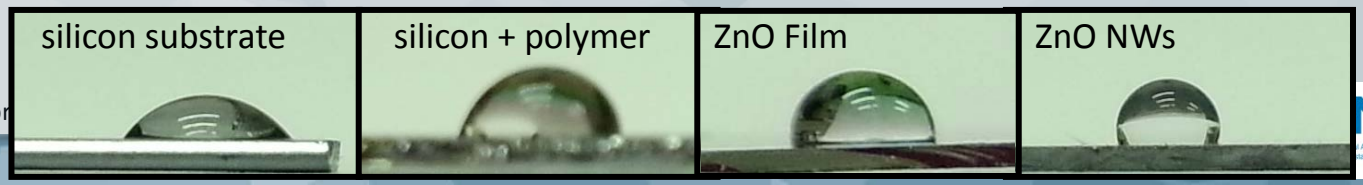

PART 2 Residual Stress and In-Situ Characterization

IN-SITU TESTING: THE CASE ON ZnO NWs

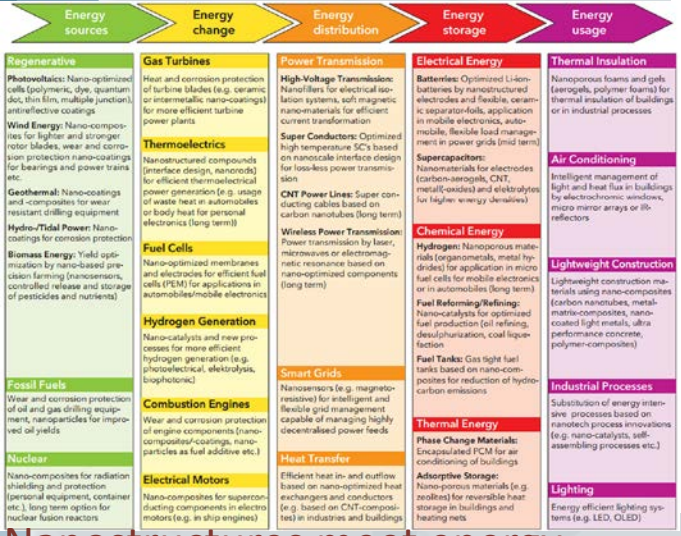

IoT: A smart world of sensors

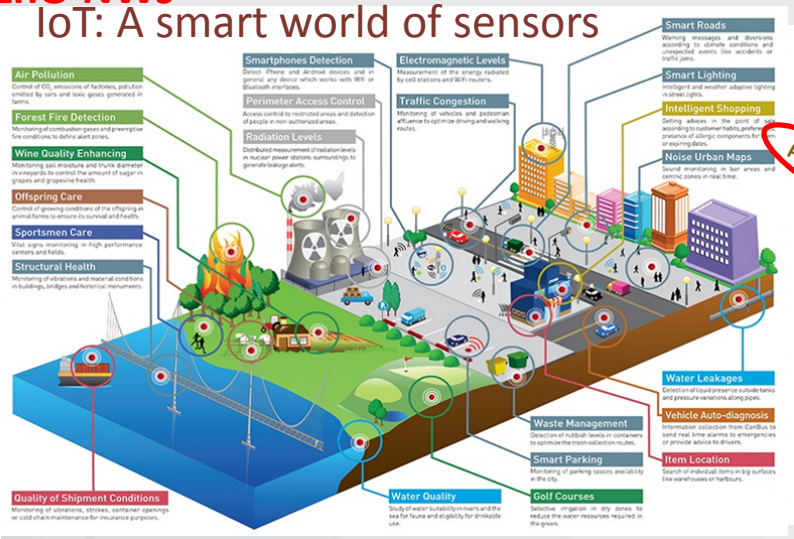

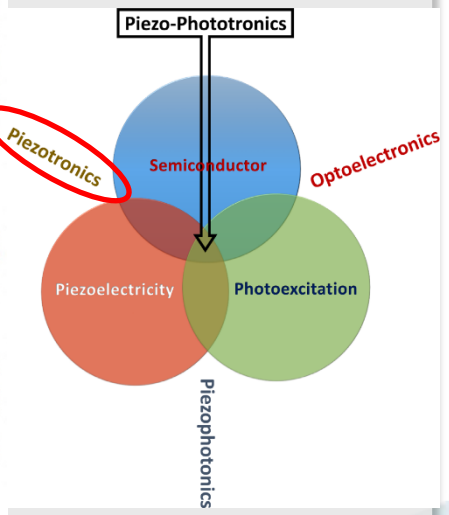

Nanostructures meet energy

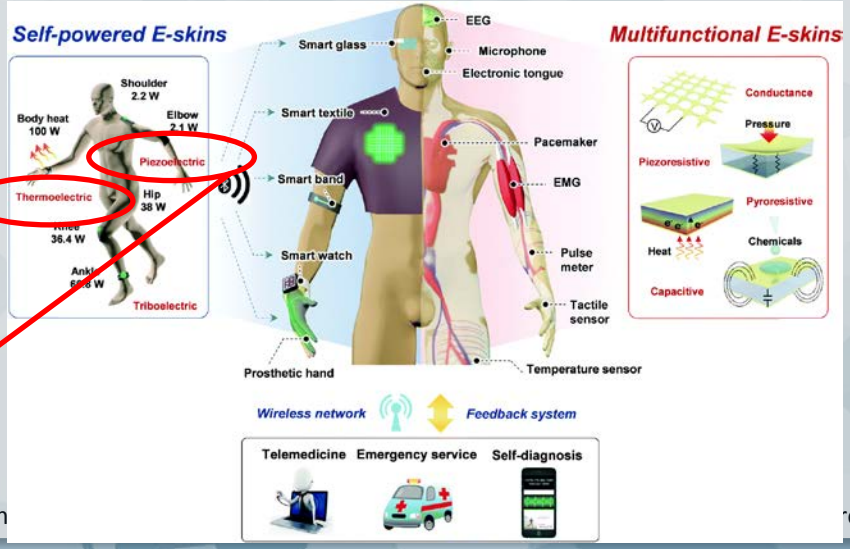

ZnO

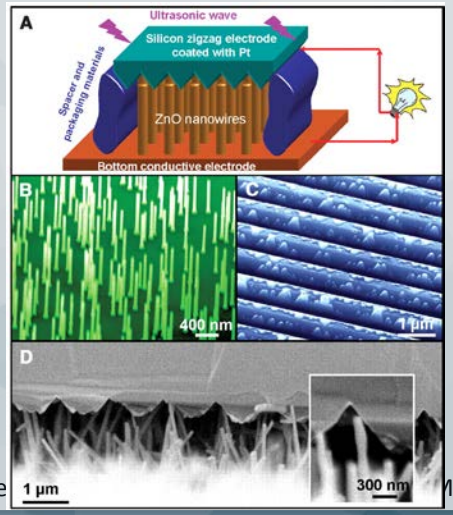

Record peak open-circuit voltage 58V and short-circuit current 134 µA. Maximum power density 0.78 W/cm³.

PART 2 Residual Stress and In-Situ Characterization

IN-SITU TESTING: THE CASE ON ZnO NWs

The change in band structure leads to the piezoresistance effect, which is a non-polar and symmetric effect

The piezotronic effect is a polar asymmetric effect

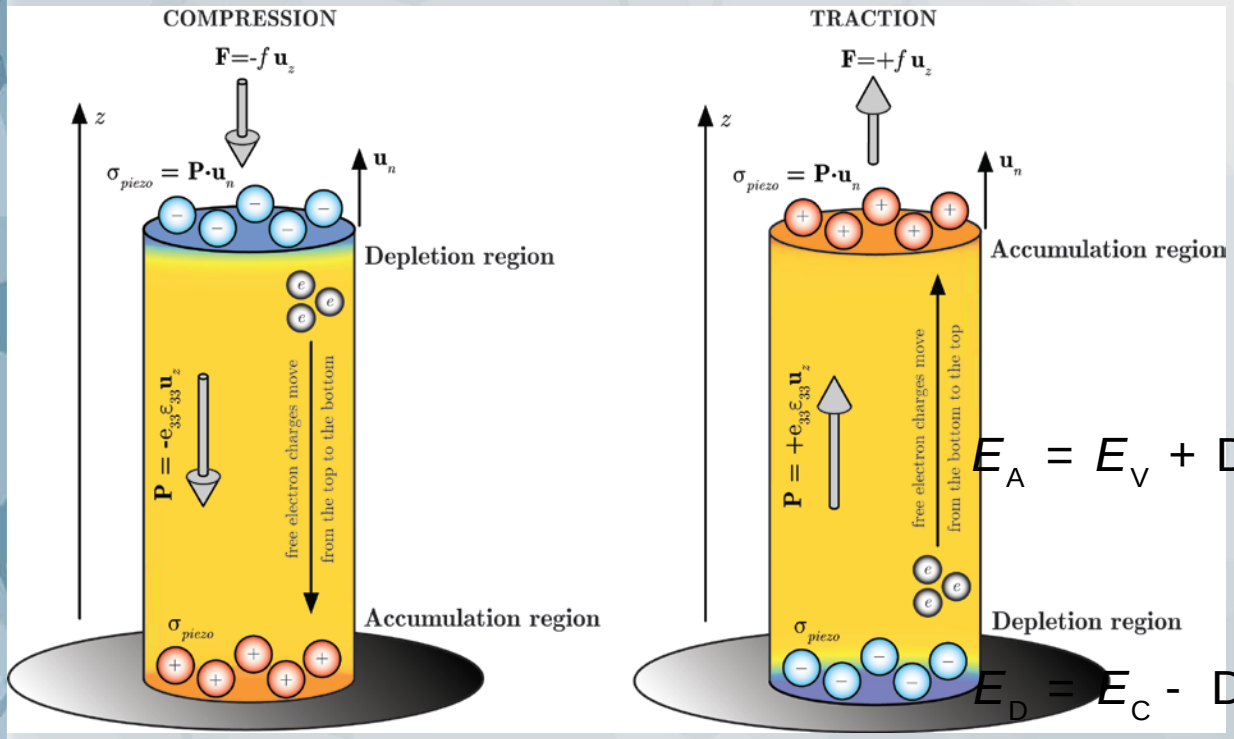

$$E_A = E_V + DE_A$$

$$E_D = E_C - DE_D$$

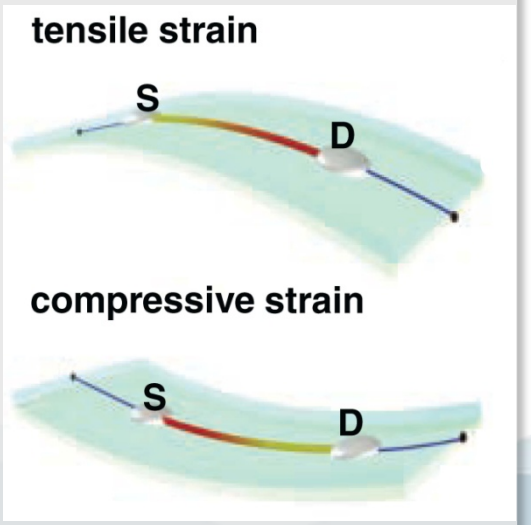

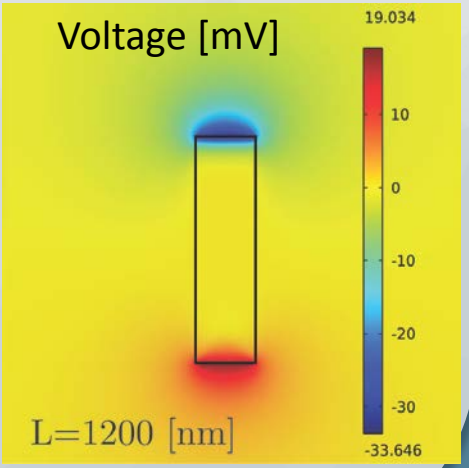

PART 2 Residual Stress and In-Situ Characterization

IN-SITU TESTING: THE CASE ON ZnO NWs

The equations are fully coupled by the constitutive equations relating mechanical, electrical and thermal quantities in piezoelectric media

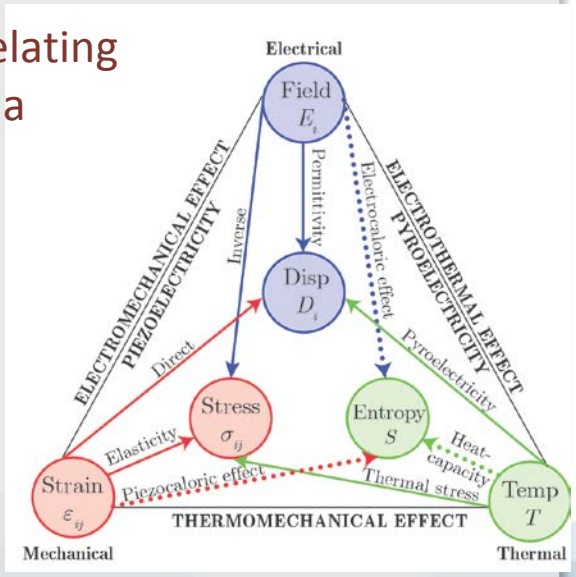

inverse piezoelectric effect

mechanical stiffness tensor

relative permittivity matrix

$$s_{ij} = C_{ijkl} e_{kl} - e_{kji} E_k - b_{ij} q$$

$$D_i = e_{ijk} e_{jk} + k_0 k_{ij} E_j + g_i q$$

piezoelectric strain tensor

primary pyroelectric coefficient vector

$$P_i^{pyro,I} = g_i q$$

tensor of stress-temperature moduli

thermal expansion tensor

$$\beta_{ij} = C_{lmij} \alpha_{lm}$$

$$P_i^{pyro,II} = e_{ijk} a_{jk} q$$

PART 2 Residual Stress and In-Situ Characterization

IN-SITU TESTING: THE CASE ON ZnO NWs

$$\sigma_{ij,i} = 0 \qquad D_{i,i} = q\left(N_{\mathrm{D}}^{+} + p - N_{\mathrm{A}}^{+} - n\right)$$

$$\sigma_{ij} = C_{ijkl}\varepsilon_{kl} - e_{kji}E_k - \beta_{ij}\theta \qquad D_i = e_{ijk}\varepsilon_{jk} + \kappa_0\kappa_{ij}E_j + \gamma_i\theta$$

due to the inverse effects

due to the direct effects

Secondary pyroelectric effect

$$f_{vi}^{\mathrm{piezo}} = \sigma_{ij,j}^{\mathrm{piezo}} \qquad \sigma_{ij}^{\mathrm{piezo}} = -e_{kji}E_k$$

$$\rho_{\mathrm{piezo}} = -P_{i,i}^{\mathrm{piezo}} \qquad P_i^{\mathrm{piezo}} = e_{ijk}\varepsilon_{jk}$$

$$f_{vi}^{\mathrm{pyro}} = \sigma_{ij,j}^{\mathrm{pyro}} \qquad \sigma_{ij}^{\mathrm{pyro}} = -\beta_{ij}\theta$$

$$\rho_{\mathrm{pyro,I}} = -P_{i,i}^{\mathrm{pyro,I}} \qquad P_i^{\mathrm{pyro,I}} = \gamma_i\theta$$

$$\left(C_{ijkl}e_{kl}\right)_{,j} + f_{vi}^{\mathrm{piezo}} + f_{vi}^{\mathrm{pyro}} = 0 \qquad \left(k_0 k_{ij}E_j\right)_i = q\left(N_{\mathrm{D}}^{+} + p - N_{\mathrm{A}}^{+} - n\right) + r_{\mathrm{piezo}} + r_{\mathrm{pyro,I}}$$

PART 2 Residual Stress and In-Situ Characterization

THE WURTZITE CRYSTAL STRUCTURE

The elastic stiffness matrix is given by:

$$\mathbf{C} = \begin{pmatrix} c_{11}^w & c_{12}^w & c_{13}^w & 0 & 0 & 0 \\ c_{12}^w & c_{11}^w & c_{13}^w & 0 & 0 & 0 \\ c_{13}^w & c_{13}^w & c_{33}^z & 0 & 0 & 0 \\ 0 & 0 & 0 & c_{44}^w & 0 & 0 \\ 0 & 0 & 0 & 0 & c_{44}^w & 0 \\ 0 & 0 & 0 & 0 & 0 & c_{66}^w \end{pmatrix}$$

where c_{ij}^w are the elastic stiffness constants with $c_{66}^w = (c_{11}^w - c_{12}^w)/2$ and the superscript w is used to refer to a wurtzite material.

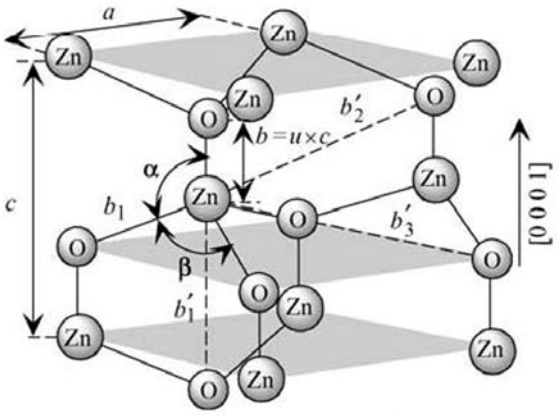

Schematic representation of a wurtzitic ZnO structure with lattice constants *a* in the basal plane and *c* in the basal direction, *u* parameter, which is expressed as the bond length or the nearest-neighbor distance *b* divided by *c* (0.375 in ideal crystal), α and β (109.47° in ideal crystal) bond angles, and three types of second-nearest-neighbor distances b'_1, b'_2, and b'_3.

The piezoelectric coupling matrix is given by

$$\mathbf{e} = \begin{pmatrix} 0 & 0 & 0 & 0 & e_{15}^w & 0 \\ 0 & 0 & 0 & e_{15}^w & 0 & 0 \\ e_{31}^w & e_{31}^w & e_{33}^w & 0 & 0 & 0 \end{pmatrix}$$

the dielectric matrix is given by

$$\begin{bmatrix} e_{11} & 0 & 0 \\ 0 & e_{22} & 0 \\ 0 & 0 & e_{33} \end{bmatrix} = \begin{bmatrix} k_{11} & 0 & 0 \\ 0 & k_{22} & 0 \\ 0 & 0 & k_{33} \end{bmatrix}$$

Tensor components	11=22	12	13=23	33	44=55
Elastic moduli C_{ij} [GPa]	209.7	121.1	105.1	210.9	42.47
Relative electric permittivity k_{ij}	7.77			8.91	
Thermal expansion tensor a_{ij} [10^{-6} K^{-1}]	4.75			2.9	
Pyroelectric tensor g_{ij} [10^{-6} C/(m^2 K)]				-12	
Thermal conductivity tensor k_{ij} [W/(m K)]	18			18	

Tensor components	31=32	33	15=24
Piezoelectric constants e_{ij} [C/m^2]	-0.51	1.22	-0.45

PART 2 Residual Stress and In-Situ Characterization

IN-SITU TESTING: THE CASE ON ZnO NWs

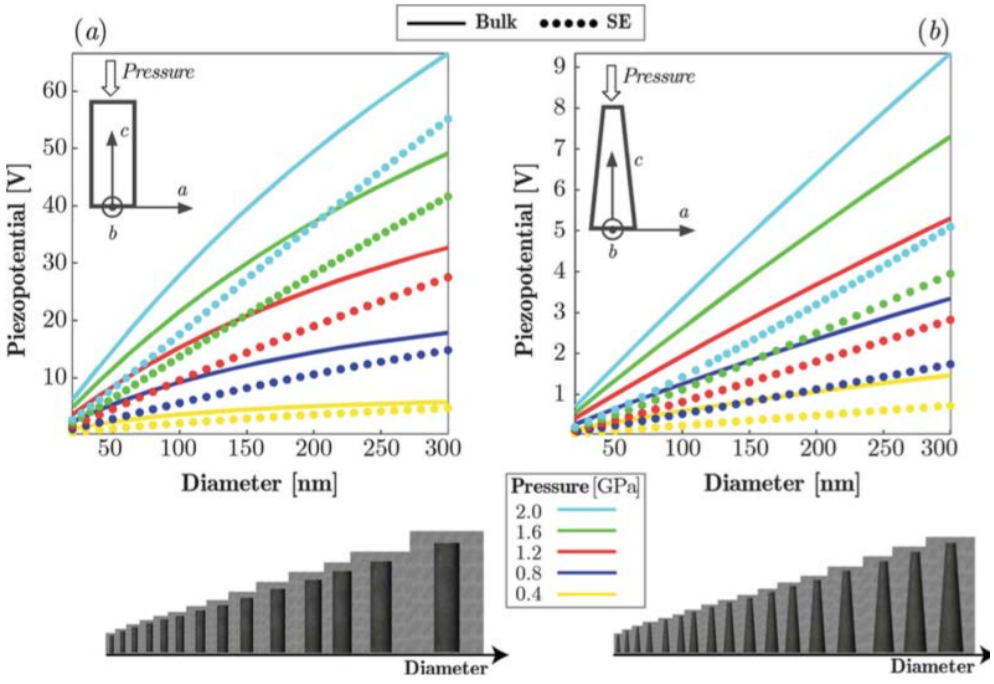

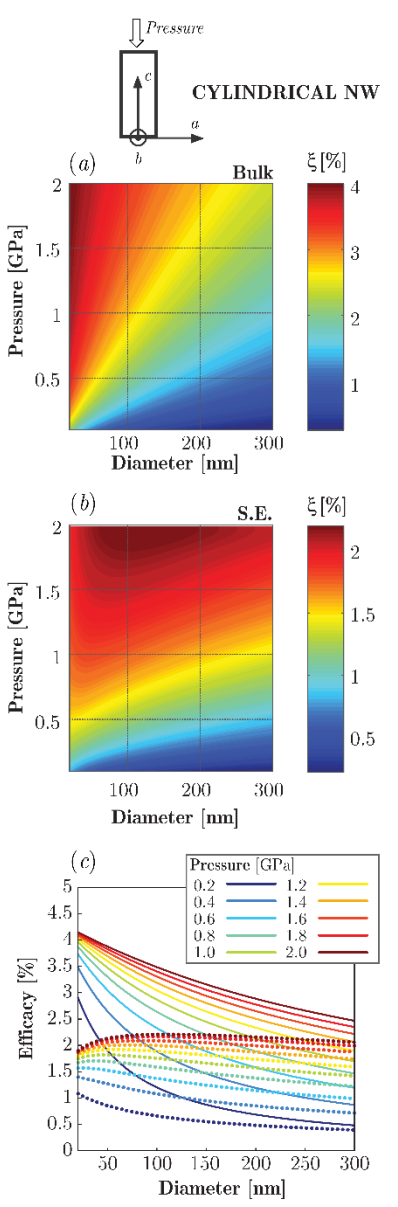

PART 2 Residual Stress and In-Situ Characterization

IN-SITU TESTING: THE CASE ON ZnO NWs

1) WET GROWN ZnO NWs

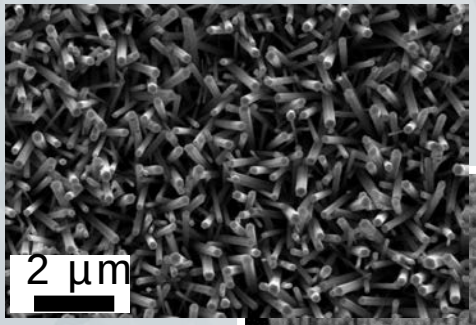

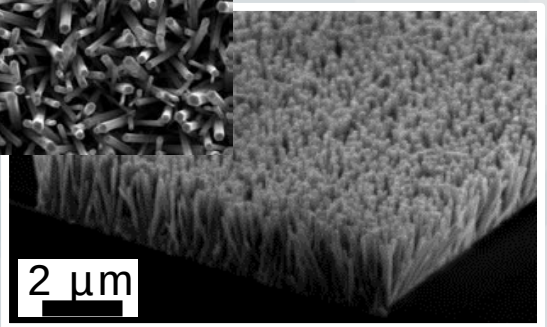

Single NW electrical characterization

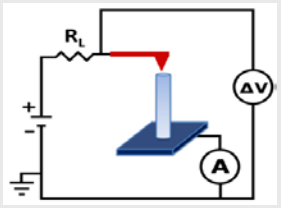

Current map

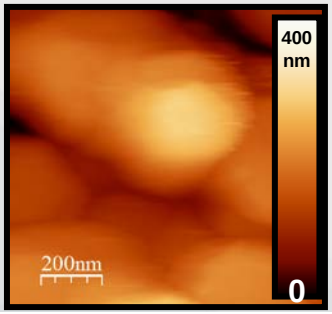

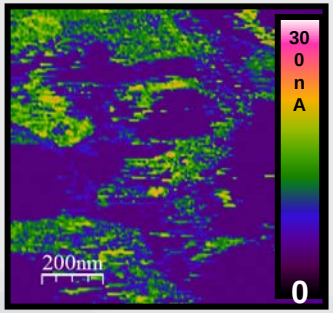

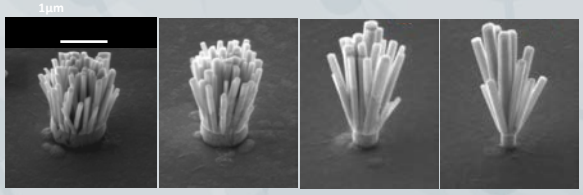

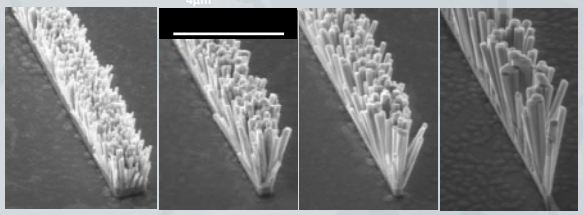

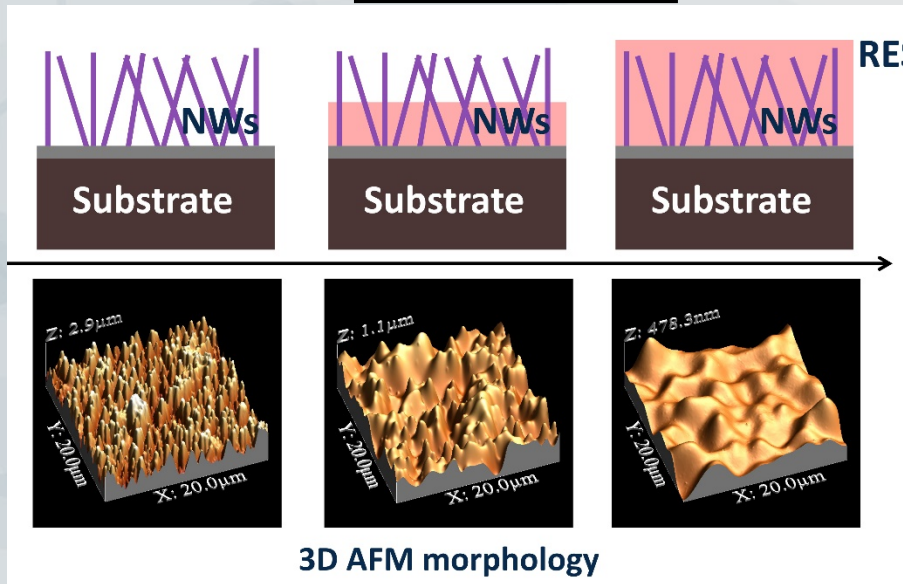

3D AFM morphology

2) RESIST COVERAGE

PART 2 Residual Stress and In-Situ Characterization

IN-SITU TESTING: THE CASE ON ZnO NWs

3) DEVICE

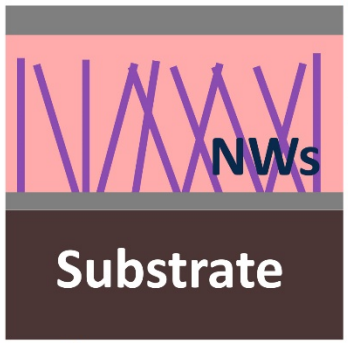

Top metal layer

NWs embedded in PMMA

Ohmic bottom metal

Device structure

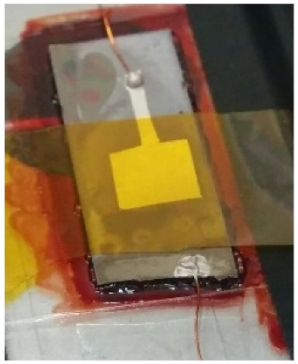

ZnO NWs harvesting device

4) MEASUREMENTS

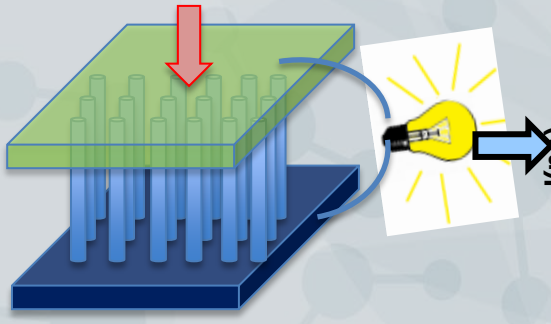

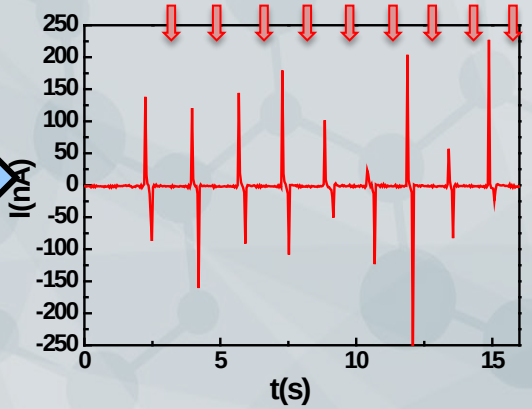

Short circuit current peaks

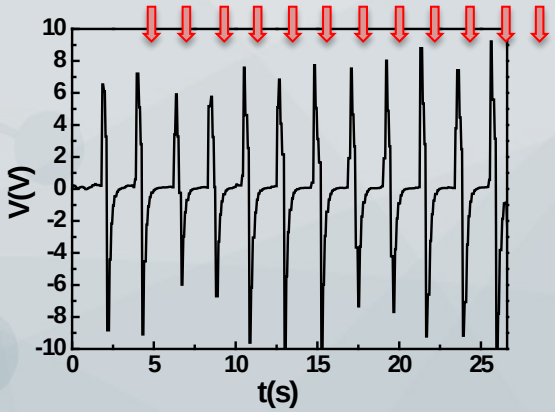

Open circuit voltage peaks

PART 2 Residual Stress and In-Situ Characterization

IN-SITU TESTING: THE CASE ON ZnO NWs

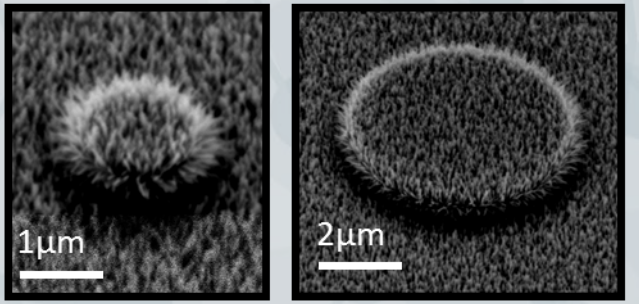

antonio.rinaldi@enea.it

CONCLUSIONS PART 2 & THANKS

NANOMECHANICS

- You need it for residual stress measurements and mechanical testing
- You need it for size effects evaluation and nanoscale exploration

antonio.rinaldi@enea.it

Thank you!

The ICARUS project has received funding from the European Union's Horizon 2020 research and innovation programme under grant agreement No 713514.

The SUPERMAT project has received funding from the European Union's Horizon 2020 research and innovation programme under grant agreement No 692216.

This document and all information contained herein is the sole property of the ICARUS and SUPERMAT Consortiums or the company referred to in the slides. It may contain information subject to Intellectual Property Rights. No Intellectual Property Rights are granted by the delivery of this document or the disclosure of its content.
Reproduction or circulation of this document to any third party is prohibited without the written consent of the author(s).
The statements made herein do not necessarily have the consent or agreement of the ICARUS and SUPERMAT consortiums and represent the opinion and findings of the author(s).

The dissemination and confidentiality rules as defined in the Consortium agreement apply to this document.

All rights reserved ®